Eur. Phys. J. D **46**, 129–150 (2008)
DOI: 10.1140/epjd/e2007-00305-4

THE EUROPEAN PHYSICAL JOURNAL D

Thermodynamic and transport properties in equilibrium air plasmas in a wide pressure and temperature range

A. D'Angola[1,a], G. Colonna[2], C. Gorse[2,3], and M. Capitelli[2,3]

[1] DIFA, Università della Basilicata, viale dell'Ateneo Lucano 10, 85100 Potenza, Italy
[2] CNR-IMIP Bari, via Amendola 122/D, 70126 Bari, Italy
[3] Dipartimento di Chimica, Università di Bari, via Orabona 4, 70126 Bari, Italy

Received 4 August 2007
Published online 23 November 2007 –

Abstract. Thermodynamic and transport properties of high temperature equilibrium air plasmas have been calculated in a wide pressure ($0.01 \div 100$ atm) and temperature range ($50 \div 60\,000$ K). The results have been obtained by using a self-consistent approach for the thermodynamic properties and higher order approximation of the Chapman-Enskog method for the transport coefficients. Debye-Hükel corrections have been considered in the thermodynamic properties while collision integrals of charge-charge interactions have been obtained by using a screened Coulomb potential. Calculated values have been fitted by closed forms ready to be inserted in fluid dynamic codes.

PACS. 52.25.Fi Transport properties – 52.25.Kn Thermodynamics of plasmas – 51.20.+d Viscosity, diffusion, and thermal conductivity

Highlight Paper

1 Symbols

a_0	Bohr radius
α	polarizability
c_p	mixture constant pressure specific heat
c_{rs}	stoichiometric coefficients of the sth species in the rth reaction
χ_s	molar fraction of sth species
$\mathcal{D}_{ij}$	binary diffusion coefficients
Δ_{DH}	Debye-Hückel correction
$\Delta\mathcal{E}_s$	energy cutoff for sth species
$\Delta\mathcal{E}_{Fs}$	Fermi energy cutoff for sth species
$\Delta\mathcal{E}_{Gs}$	Griem energy cutoff for sth species
e	Neper number
$\mathcal{E}$	mixture energy
$\mathcal{E}_s$	total mean energy of sth species
$\mathcal{E}_s^{tr}$	translational mean energy of sth species
$\mathcal{E}_s^{int}$	internal mean energy of sth species
$\mathcal{E}_{DH}$	Debye-Hückel correction to energy
ε_{si}	energy of the ith level of sth species
ϵ_0	vacuum dielectric constant
$\mathcal{F}$	mixture Helmoltz free energy
$\mathcal{F}_{DH}$	Debye-Hückel correction to Helmoltz free energy
g_{si}	statistical weight of the ith level of sth species
g_{si}^{el}	statistical weight of molecular electronic state
$\mathcal{G}$	mixture Gibbs free energy
$\mathcal{G}_{DH}$	Debye-Hückel correction to Gibbs free energy
h	Planck constant
$\mathcal{H}$	mixture enthalpy
$\mathcal{H}_{DH}$	Debye-Hückel correction to enthalpy
η	viscosity
k	Boltzmann constant
$\mathcal{K}_r^P$	equilibrium constant of rth reaction for pressure
j	rotational quantum number
$\mathcal{I}_s$	effective atomic ionization potential of sth species
$\mathcal{I}_{0s}$	unperturbed atomic ionization potential of sth species
λ	total thermal conductivity
λ_D	Debye length
$\overline{M}$	mean molar mass
m_s	mass of sth species
n	total number density of the plasma
n_s	number of internal levels of sth species
N	total particle density
N_s	particle density of sth species
$\mathcal{P}$	total pressure
$\mathcal{P}_{DH}$	Debye-Hückel correction to pressure
$\mathcal{P}_s$	partial pressure of sth species
$\mathcal{Q}_s$	total partition function of sth species
$\mathcal{Q}_s^{tr}$	translational partition function of sth species

[a] e-mail: antonio.dangola@unibas.it

$\mathcal{Q}_s^{int}$	internal partition function of sth species
q_e	electron charge
ρ	mass density of the plasma
R	ideal gas constant
R_s	name of the sth species
σ	electric conductivity
S	specific entropy
s	species index
$\mathcal{S}$	mixture entropy
$\mathcal{S}_{DH}$	Debye-Hückel correction to entropy
T	temperature
v	vibrational quantum number
z_s	charge number of sth species
$\Omega_{ij}^{(l,s)}$	collision integral of (l,s) type for interactions between species i and j

2 Introduction

Over the last decades a substantial growth in industrial applications of plasmas has occurred [1–9]. In particular, cutting, welding, spraying, metallurgy, waste destruction and surface treatment need improvements in controlling plasma processing and in understanding of flow structures and heat, mass and momentum transfer between plasma and materials. Consequently, thermodynamic properties and transport coefficients of plasmas are indispensable input data for accurate numerical modeling. In many applications it's possible to perform such calculations assuming local thermodynamic equilibrium describing the plasma with two independent state variables such as pressure and temperature. A key point is the calculation of equilibrium plasma composition necessary to determine thermodynamic and transport properties of mixtures; at this purpose a new approach has been used, based on a hierarchical solution of single reaction equilibria [10–13]. A relevant aspect in the calculation of thermodynamic properties and gas composition is the cut-off criteria used to truncate the atomic partition function, based on the pressure (Fermi criterion, see [14]) or on the plasma potential and electron density (Griem criterion [15]). In this paper, we use a combination of these criteria to have adequate cut-off for all the temperatures and pressures considered.

Transport properties are calculated using the Chapman-Enskog approximation, with a finite Sonine polynomial expansion of the Boltzmann equation up to the third order for electrons contribution to the translational thermal conductivity and for the electrical conductivity. Due to the mass difference, the heavy particles and electron Boltzmann equations are decoupled. As a consequence, the transport properties of free electrons and heavy-species are calculated independently, following the method of Devoto [16]. The collision integrals, depending on the intermolecular potentials, are continuously updated [17] to improve the calculation of transport coefficients. In this paper we have used the collision integrals reported in [17] except for the charge-charge interaction. In this case we improve the calculations updating the Liboff collision integrals [18] with the more accurate model proposed by Mason [19,20] which considers screened Coulomb potential accounting for a Debye length calculated only from the electron number density.

In this paper we improve the results presented in reference [21] for $\mathcal{P} = 1$ atm extending the pressure and temperature range. The calculation of equilibrium compositions and thermodynamic properties has been improved considering also non ideal gas effects following Debye-Hückel theory [22].

For the air mixture, the following species were considered: N_2, N_2^+, N, N^+, N^{2+}, N^{3+}, N^{4+}, O_2, O_2^+, O_2^-, O, O^-, O^+, O^{2+}, O^{3+}, O^{4+}, NO, NO^+ and e^-. Comparisons with experimental values of Asinovsky et al. [23] and Schreiber et al. [24], with theoretical values obtained by Capitelli et al. [21], Murphy [25], Hansen [26], Nicolet et al. [27] with the tables of Yos [28], all of these performed at atmospheric pressure, and with Bacri et al. [29,30] are reported. Analytical expressions of molar fractions, thermodynamic properties and transport coefficients have been reported for pressures varying from 0.01−100 atm and in the temperature range 50−60 000 K.

3 Method of calculation

The results here presented are obtained in three steps: in the first step the calculation of plasma composition has been performed varying temperature and pressure, in the second the knowledge of the composition has permitted the determination of thermodynamic properties and in the last step transport properties have been calculated using the Chapman-Enskog approximation.

Chemical equilibrium compositions and internal energy are the input for the calculation of transport coefficients. A new approach has been used for accurate evaluation of equilibrium compositions [10,11] taking into account Debye-Hückel corrections. Transport coefficients are calculated using the high order approximation of the Chapman-Enskog method [31,32]. A brief description of the model is given in the following.

3.1 Thermodynamics

To calculate thermodynamic properties of a plasma, the knowledge of partition functions, their derivatives, and the concentrations of various species present in the plasma is a prerequisite. The partition functions can be expressed as the product of the translational and internal contributions

$$\mathcal{Q}_s = \mathcal{Q}_s^{tr}\,\mathcal{Q}_s^{int} \tag{1}$$

and, as a consequence, the mean energy is given by the sum of the two contributions

$$\mathcal{E}_s = \mathcal{E}_s^{tr} + \mathcal{E}_s^{int}. \tag{2}$$

The translational partition function and the associated energy are given by [22,33]

$$\mathcal{Q}_s^{tr} = \frac{e}{N_s}\left(\frac{2\pi m_s kT}{h^2}\right)^{\frac{3}{2}} \tag{3}$$

$$\mathcal{E}_s^{tr} = \frac{3}{2}kT \tag{4}$$

while the internal partition function and the internal energy are calculated as the sum over atomic or molecular levels

$$\mathcal{Q}_s^{int} = \sum_{i=0}^{n_s} g_{si} \exp\left(-\frac{\varepsilon_{si}}{kT}\right) \tag{5}$$

$$\mathcal{E}_s^{int} = \frac{1}{\mathcal{Q}_s^{int}} \sum_{i=0}^{n_s} g_{si}\varepsilon_{si} \exp\left(-\frac{\varepsilon_{si}}{kT}\right). \tag{6}$$

For air molecules, n_s has been restricted to the bound electronic states originating by the spin and angular momentum coupling of valence electrons. Each bound state supports a finite number of ro-vibrational levels as described in references [33,34]. The partition function is calculated as

$$\mathcal{Q}_s^{int} = \sum_{i}^{n_s} \sum_{v}^{V_{max,i}} \sum_{j}^{J_{max,iv}} g_{sivj} \exp\left(-\frac{\varepsilon_{sivj}}{kT}\right). \tag{7}$$

The statistical weight of a (ivj) state depends only on the electronic and rotational contributions

$$g_{sivj} = g_{si}^{el}(2j+1). \tag{8}$$

The calculation of energy of ro-vibrational states is based on the 2D polynomial expansion on $v+\frac{1}{2}$ and $j(j+1)$ as reported on [33,35,36].

For atomic species, n_s is infinite, making the atomic internal partition functions divergent [37], as a consequence of the rapid growing of the statistical weight (i.e. for hydrogen atoms, $g_n \propto n^2$, being n the principal quantum number). This behavior is true only for isolated atoms, while interactions with other particles limit the number of levels introducing the energy cutoff $\Delta\mathcal{E}_s$ which modifies the unperturbed ionization $\mathcal{I}_{0s}$ potential as

$$\mathcal{I}_s = \mathcal{I}_{0s} - \Delta\mathcal{E}_s. \tag{9}$$

In the previous paper [21], the cutoff was fixed ($\Delta\mathcal{E}_s = 500\ \mathrm{cm}^{-1}$) using tables from reference [38]. In the present paper, we determine the cutoff self-consistently with the composition. At this purpose, the number of levels should be large enough to make effective the contribution of the cutoff, while in available databases [39,40] the levels reported are not sufficient to fulfill this condition. Therefore the atomic data in [39] have been extended by Ritz-Rydberg series (for detail see [33,34]).

To determine the self-consistent cutoff, two different approaches have been considered: the Fermi criterion [41,42], which compares the mean distance with the atomic radius

$$\Delta\mathcal{E}_{Fs} = \frac{a_0}{z_s+1} N^{\frac{1}{3}} \tag{10}$$

under the hypothesis of hydrogenoid levels and for high energy states and the Griem criterion [15] which considers the contribution of plasma potential

$$\Delta\mathcal{E}_{Gs} = \frac{z_s+1}{4\pi\epsilon_0\lambda_D} \tag{11}$$

where λ_D is the Debye length

$$\lambda_D = \sqrt{\frac{\epsilon_0 kT}{Nq_e^2\sum_s z_s^2\chi_s}}. \tag{12}$$

The cutoff selected is the largest between the Fermi and Griem values

$$\Delta\mathcal{E}_s = \max\left(\Delta\mathcal{E}_{Fs}, \Delta\mathcal{E}_{Gs}\right). \tag{13}$$

It must be noted that the Griem cutoff depends on the plasma composition making necessary a self-consistent solution of the problem.

The formation of the plasma potential induces in the system real gas properties. The corrections to the perfect gas behavior have been determined in the framework of the Debye-Hückel theory [22]

$$\Delta_{DH} = \frac{kT}{24\pi\lambda_D^3} \tag{14}$$

$$\mathcal{P}_{DH} = -\Delta_{DH} \tag{15}$$

$$\mathcal{F}_{DH} = -2V\Delta_{DH} \tag{16}$$

$$\mathcal{G}_{DH} = \mathcal{E}_{DH} = \frac{3}{2}\mathcal{F}_{DH} \tag{17}$$

$$\mathcal{H}_{DH} = 2\mathcal{F}_{DH} \tag{18}$$

$$\mathcal{S}_{DH} = \frac{1}{2}\mathcal{F}_{DH}. \tag{19}$$

It must be noted that there is also a correction to the pressure leading to the result

$$\mathcal{P} = \sum_s \mathcal{P}_s + \mathcal{P}_{DH} \tag{20}$$

where $\mathcal{P}_s$ follows the perfect gas role

$$\mathcal{P}_s = N_s kT. \tag{21}$$

The partial pressures are calculated solving the equilibrium equation system. Given a reaction

$$\sum_s c_{rs} R_s = 0 \tag{22}$$

the sum running over all the species, where the reactants have negative coefficients, the products have positive coefficients and species not involved in the reaction have null coefficients, its equilibrium equation can be written as

$$\mathcal{K}_r^P = \prod_s \mathcal{P}_s^{c_{rs}}. \tag{23}$$

In a mixture, there are many of such reactions and the equilibrium composition is obtained solving the system of nonlinear coupled equilibrium equations. The determination of equilibrium composition is a complex problem and many algorithms have been developed. We have applied a new approach [10,11] which consists in solving one equilibrium equation at a time. The method is based on the idea of Villars [12,13] soon abandoned because

the method was not easily automatized. The reaction ordering is chosen determining, at each step, which reaction is farther from equilibrium, defining a reaction distance. The algorithm is very fast and stable and details can be found in [10,11]. The method finds in very few steps the concentration of principal species, refining the solution of minority species in a second stage. Once each reaction is solved, Debye length and cutoffs are updated. The cutoff converges faster than the mixture composition, being related to the concentration of the majority species. In hierarchical methods, the concept of accuracy differs completely respect to global minimization approaches, where the tolerance is the maximum percentage error for each concentration. In fact the concentrations precision is given by the machine error for all the species except for those with molar fraction below a given tolerance which are affected by large errors. Details about error analysis are reported in [11].

The thermodynamic properties (per unit volume) of the mixture are calculated using the traditional transformation equation from energy or partition function

$$\mathcal{F} = -kT \sum_s N_s \ln \mathcal{Q}_s + \mathcal{F}_{DH} \tag{24}$$

$$\mathcal{E} = -\sum_s N_s \mathcal{E}_s + \mathcal{E}_{DH} \tag{25}$$

$$\mathcal{H} = \mathcal{E} + \mathcal{P} \tag{26}$$

$$\mathcal{G} = \mathcal{F} + \mathcal{P} \tag{27}$$

$$\mathcal{S} = \frac{\mathcal{E} - \mathcal{F}}{T} \tag{28}$$

$$c_p = \left(\frac{d\mathcal{H}}{dT}\right)_{\mathcal{P}}. \tag{29}$$

It should be noted that virial corrections have been neglected in our calculations. Different works [43,44] have shown that the virial corrections to thermodynamic properties are very small (within few percent) for $T > 2000$ K up to 1000 atm. Virial corrections can be however important for very low temperatures ($T < 300$ K) and very high pressures ($\mathcal{P} \sim 100$ atm) [45] i.e. far from plasma conditions.

3.2 Collision integrals of air species

In the present paper a recent compilation of collision integrals obtained by Capitelli et al. [17] has been used in order to calculate transport properties, except for interactions between charged species. For these interactions, the model proposed by Mason [19,20] has been applied. Mason approach considers screened Coulomb potential accounting for a Debye length calculated only from the electron number density.

Transport coefficients are strongly dependent on the collision integrals, obtained averaging over a Maxwellian distribution the collision cross-sections for pairs of species. The collision integrals for interactions between species i and j are defined by [31,32]

$$\Omega_{ij}^{(l,s)} = \sqrt{\frac{kT}{2\pi\mu_{ij}}} \int_0^{+\infty} \exp(-\gamma_{ij}^2)\gamma_{ij}^{2s+3} Q_{ij}^{(l)}(\gamma_{ij})\, d\gamma_{ij} \tag{30}$$

where μ_{ij} is the reduced mass, γ_{ij} the reduced initial relative speed of the colliding molecules and $Q_{ij}^{(l)}$ the gas-kinetic cross-sections. These quantities are defined as follows

$$\gamma_{ij} = \sqrt{\frac{\mu_{ij}}{2kT}} u_{ij} \tag{31}$$

$$Q_{ij}^{(l)}(\gamma_{ij}) = 2\pi \int_0^{+\infty} \left(1 - \cos^l \chi\right) b db \tag{32}$$

where u_{ij} is the initial relative velocity of two molecules in a binary encounter, b the impact parameter and χ the deflection angle, which is a function of b, γ_{ij} and the intermolecular potential $V(r)$, where r is the separation between the interacting particles. Therefore the calculation of $\Omega_{ij}^{(l,s)}$ reduces to the knowledge of $V(r)$.

In order to calculate collision integrals corresponding to interactions between neutral species an exponential repulsive form has been used for $T > 2000$ K

$$V(r) = \varphi_0 \exp(-r/\rho) \tag{33}$$

where ρ and φ_0 are parameters obtained fitting the experimental studies of Leonas [46] for the interactions N_2–N_2, N_2–N, N_2–O_2, N_2–O, N_2–NO, N–O_2, N–NO, O_2–O_2, O_2–O, O_2–NO, O–NO, NO–NO and of Riabov [47] for N–O. For the interactions N_2–N_2, N_2–N, N_2–O_2, N_2–O, N_2–NO, N–O_2, N–O, N–NO, O_2–O_2, O_2–O, O_2–NO, O–NO, NO–NO and for $T < 1000$ K a Lennard-Jones potential has been considered

$$V(r) = 4V_0 \left[\left(\frac{\sigma}{r}\right)^{12} - \left(\frac{\sigma}{r}\right)^{6}\right] \tag{34}$$

where V_0 is the depth of the potential well and σ the collision diameter for the interactions. The parameters V_0 and σ are tabulated in [17].

For the interaction N–N an average over 4 potential curves (bound and repulsive) spectroscopically denoted by ${}^1\Sigma$, ${}^3\Sigma$, ${}^5\Sigma$, ${}^7\Sigma$ and over 18 different potentials in the case of O–O have been considered. The statistical weights to be used in the averages are equal to the spin multiplicity for Σ states and two times the spin multiplicity for Π, Δ, ... states. Bound states have been treated according to a Morse potential

$$V(r) = V_0 \left\{\exp\left[-2a\left(r - r_e\right)\right] - 2\exp\left[-a\left(r - r_e\right)\right]\right\} \tag{35}$$

where r_e, V_0 and a, tabulated in [17], are respectively the equilibrium bond distance, the depth of the potential well and a constant value related to the width of the well. The repulsive ones have been treated according to equation (33). For $T < 1000$ K a Lennard-Jones potential has been used [48].

Table 1. Coefficients to calculate collision integrals between charged particles by using equation (38).

	c_6	c_5	c_4	c_3	c_2	c_1	c_0
$\Omega^{(1,1)*a}$	−6.8907164e-7	3.9962681e-5	−9.1726603e-4	1.1119743e-2	−8.6680553e-2	–1.4201786	−7.9206301e-1
$\Omega^{(1,1)*r}$	4.5117138e-7	−1.8071172e-5	1.0779533e-4	4.6897082e-3	−9.5164062e-2	−1.1924897	−1.3985613
$\Omega^{(1,2)*a}$	−5.7227070e-7	3.2934374e-5	−7.4777692e-4	8.9360011e-3	−6.8914896e-2	−1.5259733	−1.4388180
$\Omega^{(1,2)*r}$	1.8550098e-7	−2.9457724e-6	−2.0524258e-4	7.2736296e-3	−9.6108844e-2	−1.3028643	−1.8990738
$\Omega^{(1,3)*a}$	−4.3210796e-7	2.5069749e-5	−5.7744446e-4	7.0875826e-3	−5.7252758e-2	−1.5798792	−1.9240126
$\Omega^{(1,3)*r}$	−4.9754626e-8	9.4148622e-6	−4.3259106e-4	8.7680260e-3	−9.3477251e-2	−1.3767661	−2.2877081
$\Omega^{(2,2)*a}$	−7.3601073e-7	4.6128777e-5	−1.1591771e-3	1.5291388e-2	−1.2062283e-1	−1.3061990	−8.1198723e-1
$\Omega^{(2,2)*r}$	3.7088651e-7	−1.2368963e-5	−4.3287839e-5	6.4520586e-3	−1.0180688e-1	−1.2242632	−1.1096929
$\Omega^{(2,3)*a}$	−9.9732643e-7	5.8539823e-5	−1.3501321e-3	1.5966952e-2	−1.1181856e-1	−1.3939960	−1.2004374
$\Omega^{(2,3)*r}$	1.3746615e-7	4.8295307e-8	−2.7706436e-4	8.0837639e-3	−1.0007200e-1	−1.2999675	−1.4700797

In the case of ion-neutral non-resonant interactions, collision integrals have been calculated by using a polarizability model which assume the following closed form [17]

$$\Omega^{(i,j)} = a_{ij} z \left(\frac{\alpha}{T}\right)^{1/2} \tag{36}$$

where a_{ij} is a coefficient depending on the order (i,j) of collision integrals, z is the ion charge and α is the polarizability [49]. For N^+–O and N–O^+ interactions, collision integrals calculated by Stallcop and Partridge have been used [50,51]. In the case of ion-neutral resonant collisions (N_2^+–N_2, N^+–N, O_2^+–O_2, O_2^-–O_2, O–O^-, O–O^+, NO–NO^+) diffusion and viscosity type collision integrals have been distinguished. For N^+–N and O–O^+, interactions, the viscosity-type collision integrals have been calculated using Morse and repulsive potentials [52] and considering that the interactions occur through 12 potential curves ($^{2,4,6}\Sigma_{g,u}^+$; $^{2,4,6}\Pi_{g,u}^{2,4,6}$) in the case of N^+–N, while through 24 potential curves [53] for O–O^-. In the case of NO–NO^+, N_2^+–N_2, O_2^+–O_2, O_2^-–O_2 a polarizability model has been used.

The collision integrals diffusion type for N^+–N and O–O^+ interactions have been obtained considering that the diffusion cross section $Q^{(1)}$ is dominated at high temperature by charge transfer [54,55] and at low temperature by the polarizability. The dependence of the charge-transfer cross section on relative velocity v is given by

$$Q^{(1)} = \left[C - D \log\left(v\right)\right]^2 \tag{37}$$

where C and D have been calculated from experimental measurements [54,55]. Diffusion type collision integrals for N_2^+–N_2, O_2^+–O_2, O_2^-–O_2, O–O^-, NO–NO^+ interactions have been calculated simply by charge transfer cross sections [55,56].

Collision integrals for e^-–N_2 and e^-–O_2 interactions have been calculated numerically by using the momentum transfer cross section reported by Phelps and Pitchford [57,58] and by referring to the works of Chandra et al. [59] and Shyn et al. [60]. In the case of e^-–N, the momentum transfer cross section selected is the one reported by Capitelli and Devoto [52] corrected by referring to the work of Thompson [61], while for the calculation of e^-–O collision integrals, the $Q^{(1)}$ and $Q^{(2)}$ evaluated by Thomas et al. [62] and the differential cross sections of Blaha et al. [63] have been used.

For minor interactions, N–N^{n+}, N_2–N^{n+}, O–O^{n+}, O_2–O^{n+}, O^+–N_2, N^+–O_2, N_2^+–NO, O_2^+–NO, O^+–NO, N^+–NO a polarizability model (Eq. (36)) for both diffusion and viscosity-type collision integrals has been used.

Finally, accurate collision integrals for interactions between charged particles have been obtained by using the model proposed by Mason [19,20], where screened Coulomb potential accounting for a Debye length calculated only from the electron number density has been considered. The same assumption has been used by Devoto [64] and Murphy [65], while more recently André et al. [66] calculated the Debye length also allowing the screening effect of ions. Our choice can have no-negligible effects at very high temperature, when multi-charged ions become the predominant species.

Relevant differences in transport properties have been observed respect to results obtained by using Liboff [18] cross sections. The numerical results of Mason et al. [19,20] have been fitted by the following equations:

$$\log \Omega^* = \sum_{j=0}^{6} c_j \left[\log\left(T^*\right)\right]^j \tag{38}$$

where T^* represents the ratio of the Debye shielding distance to the particle diameter q_e^2/kT

$$T^* = \frac{\lambda_D}{(q_e^2/kT)} \tag{39}$$

and c_j are reported in Table 1 for repulsive (r) and attractive (a) reduced collision integrals in standard dimensionless notation [31]. The set of collision integrals used in this paper is in substantial agreement with the recent results reported by [67].

3.3 Transport properties

Transport properties have been calculated using the Chapman-Enskog method, with a finite Sonine polynomial expansion of the Boltzmann equation. Since electron mass is smaller than that of heavy species, the heavy-species Boltzmann equation is decoupled from that of electrons.

Therefore electron and heavy-species transport properties are calculated independently following the method of Devoto [16].

The derivation of transport coefficients to a first-order approximation requires the calculation of $\Omega_{ij}^{(1,1)}$ and $\Omega_{ij}^{(2,2)}$ while $\Omega_{ij}^{(1,2)}$ and $\Omega_{ij}^{(1,3)}$ are required to extend the calculation to a second-order approximation. For the calculation of the electrical conductivity and the electron contribution to the translational thermal conductivity $\Omega_{ij}^{(1,4)}$, $\Omega_{ij}^{(1,5)}$, $\Omega_{ij}^{(2,3)}$ and $\Omega_{ij}^{(2,4)}$ for interactions between electrons and other charged particles are also required.

The viscosity coefficient is calculated using the first-order approximation proposed by Hirschfelder et al. [31]. The contribution of the electrons to the viscosity is negligible, consequently, can be approximated in the following manner

$$\eta \cong \eta_h + \eta_e \cong \eta_h \tag{40}$$

h referring to heavy particles and e to the electrons.

The total thermal conductivity of plasma is calculated as the sum of three contributions:

$$\lambda = \lambda_{tr} + \lambda_{int} + \lambda_r \tag{41}$$

in which λ_{tr} is the translational thermal conductivity, λ_{int} the internal thermal conductivity and λ_r the reactive contribution to the total thermal conductivity. The translational contribution is calculated considering a non-reacting plasma of spherical molecules without internal degrees of freedom. Removing this hypothesis internal and reactive contributions must be added. As for the coefficient of viscosity, the translational thermal conductivity λ_{tr} can be considered as the sum of two contributions, due to the heavy particles and to the electrons [16]

$$\lambda_{tr} = \lambda_h + \lambda_e. \tag{42}$$

The contributions of the heavy and electron components to the translational thermal conductivity are calculated respectively by means of the second and third order approximations. In fact, the separation between the solutions of the electron and heavy distribution functions allows two different levels of approximations:

$$\lambda_{tr} = \lambda_h\,(2) + \lambda_e\,(3)\,. \tag{43}$$

In LTE plasma, the thermal conductivity may be considerably higher than in frozen or non-reacting mixtures. In fact, dissociation and ionization reactions in plasma increase the thermal conductivity and the heat transported as chemical enthalpy of molecules, which diffuse cause the existence of concentration gradients. In the present work, the method of Butler and Brokaw [68] has been used to calculate the contribution to the total thermal conductivity. Between the $\nu = 19$ species R_i present in the air plasma, $\mu = 16$ are combinations of a base composed of 3 independent species. The simplest base, composed of atomic species (N, O) and electrons, cannot be used in the overall temperature range because numerical problems arise when one or more concentrations become too small. For this reason the base is generated automatically selecting species with higher concentrations. At low temperature, when the ionization is too weak the dimension of the base reduces to 2 neutral elements. Each species is written as a linear combination (a chemical reaction) of the base species:

$$R_i = \sum_{j=\mu+1}^{\nu} n_{ij} R_j \quad i = 1, \ldots, \mu. \tag{44}$$

The reactive thermal conductivity has been calculated with the following formula [68]:

$$\lambda_r = \frac{1}{RT^2} \sum_{j=1}^{\nu} \Lambda_j \Delta\mathcal{H}_j \tag{45}$$

where Λ_j are the solutions of a linear system and $\Delta\mathcal{H}_i = \sum_{j=\nu+1}^{\mu} n_{ij}\mathcal{H}_j - \mathcal{H}_i$ is the heat of the ith reaction. In the calculation the species with χ_i very small (i.e. $\chi_i < 10^{-20}$) are excluded.

The presence of internal degrees of freedom affects the heat flux vector. The exact expression for the coefficient of thermal conductivity depends on the transition probabilities for the transfer of energy among the degrees of freedom of the molecules. In this work, the assumption of Eucken [69] has been used, applicable when the rate of transfer is sufficiently fast and the distribution of molecules among the various states of freedom is essentially the equilibrium distribution. The simplified expression of Eucken has been used

$$\lambda_{int} = \frac{1}{T} \sum_{j=1}^{\nu} \frac{\chi_j \frac{c_{p,int,\,j}}{R}}{\sum\limits_{i=1}^{\nu} \frac{\chi_i}{\mathcal{P}\mathcal{D}_{ij}\,(1)}} \tag{46}$$

in which $c_{p,int,\,j}$ is the internal molar specific heat at constant pressure of the jth species and $\mathcal{D}_{ij}\,(1)$ is the first approximation to the coefficient of diffusion of a binary mixture. The use of this equation for the calculation of the transport of the internal energy (electronic) of atomic species is open to questions since the electronically excited states present much higher transport cross sections than the ground state. This point has been recently analyzed by our group in the case of atomic hydrogen plasmas [70,71]. Unfortunately, the knowledge of transport cross sections of excited states for air plasma is still scanty, despite the enormous efforts of scientific community [72–76].

The electric conductivity is calculated using the third approximation proposed by Devoto [77] to compute the ordinary diffusion coefficient and neglecting the contribution of the ions to the current

$$\sigma = q_e^2 \frac{n_e m_e n}{\rho k T} \mathcal{D}_{ee} \tag{47}$$

where n and ρ represent the total number density and the mass density of the plasma. It should be noted that we have neglected the contribution of ions to the current as done in [78] for SF_6 plasma. This contribution can be relevant at high pressures and low temperatures, when the negative ions dominate. This occurs however when the molar fraction of negative ions is so small that the electrical conductivity is close to zero.

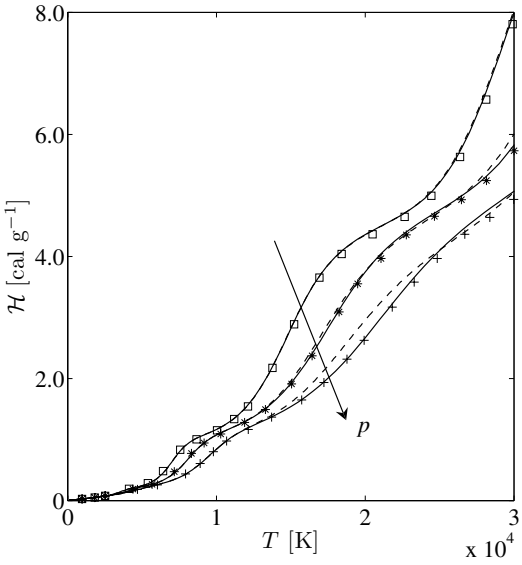

Fig. 1. Comparison of specific enthalpy at different pressures (1, 10, 100 atm): present work (full line), constant cut-off (dashed line), Bacri et al. at 1 atm (□), at 10 atm (∗) and at 100 atm (+).

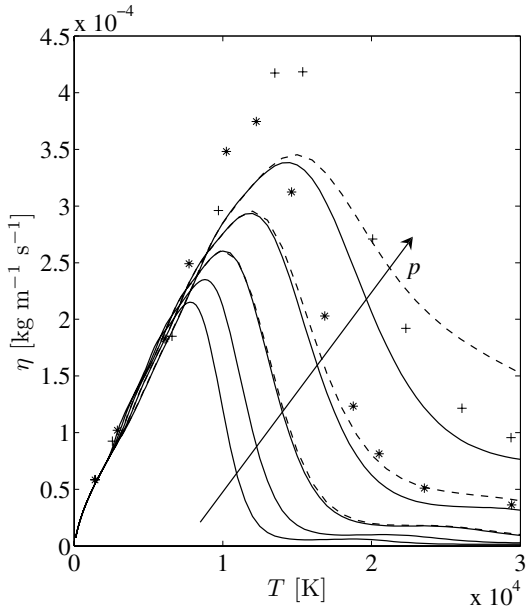

Fig. 2. Comparison of viscosity coefficient at different pressures (0.01, 0.1, 1, 10, 100 atm): present work (full line), constant cut-off (dashed line), Bacri et al. at 10 atm (∗) and at 100 atm (+).

4 Results

In the paper chemical compositions, thermodynamic and transport properties of air plasma have been calculated in the temperature range 50–60 000 K and for pressure varying from 0.01 to 100 atm. Calculated values have been fitted by analytical functions and fitting coefficients have been tabulated in Appendix.

Our results have been compared with other numerical [21,25–30] and experimental [23,24] values and comparisons have been made between results obtained considering constant cut-off and self-consistent cut-off [15].

Thermodynamic properties are in satisfactory agreement with existing data [29,30] while some differences arise at high pressure (>10 atm) when the constant cut-off is considered. Sensitivity of mixture thermodynamic properties to cut-off is much smaller than that of single species. In fact increasing the cut-off produces two opposite effects: a decrease of internal energy of atomic species and an increase of ionization energy [79]. At high pressures ionization degree reduces while, keeping constant cut-off, the internal energy doesn't change. As an example, this effect can be observed in Figure 1 where specific enthalpy has been reported with self-consistent cut-off (full line) and constant cut-off (500 cm^{-1}) and compared with theoretical results obtained by Bacri et al. [29,30]. On the other hand self-consistent cut-off produces larger differences in transport coefficients due to the different chemical equilibrium compositions obtained, especially at high pressure as shown in Figures 2, 3 and 4, where comparisons between calculated viscosity, electrical conductivity and thermal conductivity (full line) at different pressures (0.01, 0.1, 1, 10, 100 atm) have been reported with values obtained by other authors [29,30] and considering a constant cut-off (dashed line).

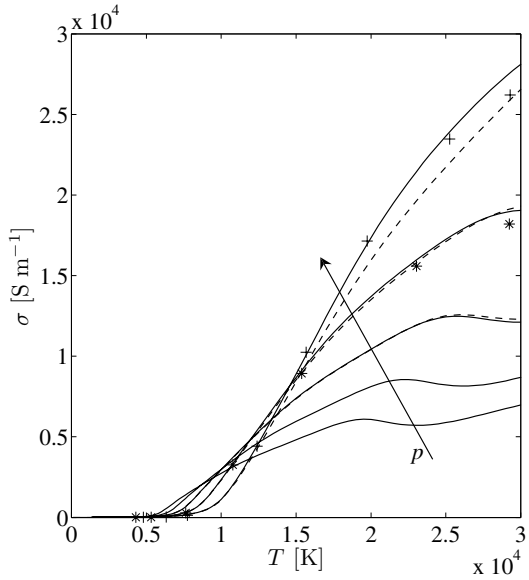

Fig. 3. Comparison of electric conductivity at different pressures (0.01, 0.1, 1, 10, 100 atm): present work (full line), constant cut-off (dashed line), Bacri et al. at 10 atm (∗) and at 100 atm (+).

In Figure 5 viscosity coefficient at atmospheric pressure has been compared with theoretical values obtained by other authors. The agreement is in general satisfactory: the small differences are due to the different set of collision integrals for heavy particles used in the calculations. Figures 6 and 7 show the electric conductivity and the total thermal conductivity (full lines) at atmospheric pressure compared with theoretical and experimental values

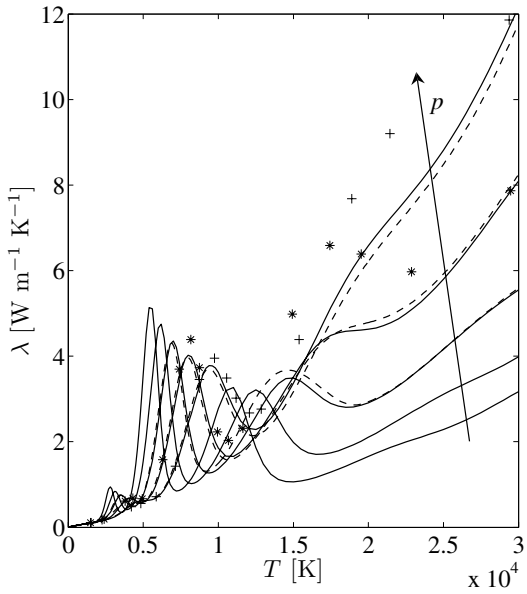

Fig. 4. Total thermal conductivity at different pressures (0.01, 0.1, 1, 10, 100 atm): present work (full line), constant cut-off (dashed line), Bacri et al. at 10 atm (∗) and at 100 atm (+).

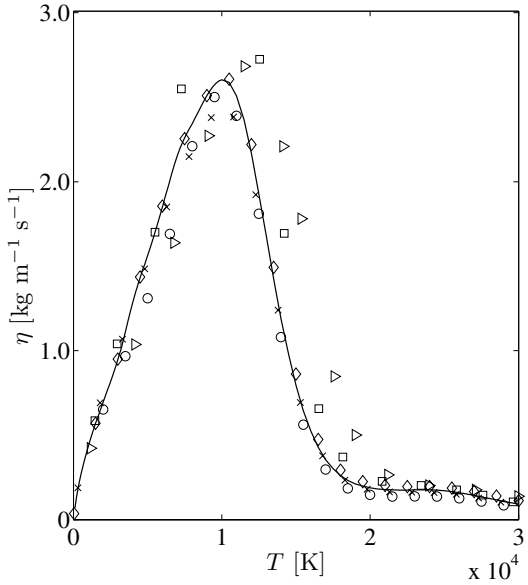

Fig. 5. Viscosity coefficient at atmospheric pressure. Results obtained in the present work (full line) are compared with those obtained by Murphy (×) [25], Yos (o) [28], Bacri (□) [30], Nicolet (▷) [27] and Capitelli et al. (◇) [21].

obtained by other authors. It is of particular interest the differences between the values obtained in the present paper with those obtained by Capitelli et al. [21] where collision integrals between charged particles have been calculated following the model of Liboff [18].

4.1 Fitting of transport and thermodynamic properties

Fitting transport coefficients and thermodynamic functions of air mixture in a wide temperature and pressure range (50−60 000 K and $10^{-2} \div 10^2$ atm) is a complex problem due to the non-monotone behavior of the relevant quantities as a function of temperature. To take into account the appearance and disappearance of the numerous species as well as the dependence of the global quantities on the actual composition, we have chosen the following functions: sigmoid, Gaussian and some special functions

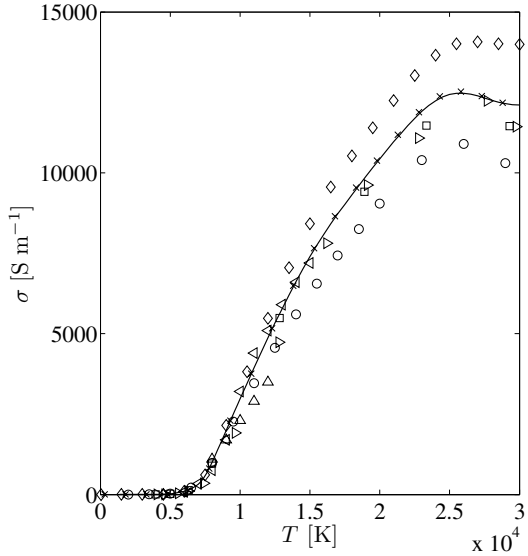

Fig. 6. Electric conductivity of air at atmospheric pressure. Results obtained in the present work (full line) are compared with those obtained by Murphy (×) [25], Yos (o) [28], Bacri (□) [30], Nicolet (▷) [27], Capitelli et al. (◇) [21], Asinovsky et al. (◁) [23] and Schreiber et al. (△) [24].

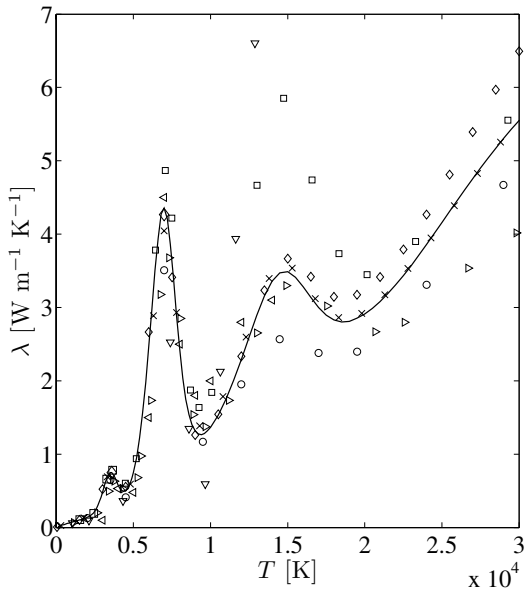

Fig. 7. Total thermal conductivity of air at atmospheric pressure. Results obtained in the present work (full line) are compared with those obtained by Murphy (×) [25], Yos (o) [28], Bacri (□) [30], Nicolet (▷) [27], Capitelli et al. (◇) [21], Hansen (▽) [26], Asinovsky et al. (◁) [23] and Schreiber et al. (△) [24].

listed below:
Gaussian

$$\gamma\left(T;c,\Delta\right)=\exp(-q^2),\quad q=\frac{T-c}{\Delta} \tag{48}$$
$$\gamma_i\left(T\right)=\gamma\left(T;c_i,\Delta_i\right).$$

Sigmoid

$$\sigma\left(T;c,\Delta\right)=\frac{\exp(q)}{\exp(q)+\exp(-q)},\quad q=\frac{T-c}{\Delta} \tag{49}$$
$$\sigma_i\left(T\right)=\sigma\left(T;c_i,\Delta_i\right).$$

Special functions

$$\xi\left(T;a,c,\Delta,w\right)=a-c\exp(-\left(T/\Delta\right)^w) \tag{50}$$
$$\xi_i\left(T\right)=\xi\left(T;a_i,c_i,\Delta_i,w_i\right)$$
$$\varphi\left(T;a,w\right)=aT^w \tag{51}$$
$$\varphi_i\left(T\right)=\varphi\left(T;a_i,w_i\right).$$

The dependence of the fitted data on the pressure has been calculated by fitting the parameters a_i, c_i, Δ_i, w_i as a function of the pressure logarithm. In particular this expression has been used

$$C=\sum_{j=0}^{n}\alpha_j x^j \tag{52}$$

where $x=\log\left(\mathcal{P}\right)$ and C represents any of the parameters a_i, c_i, Δ_i, w_i of the previous functions or its natural logarithm. The α_j coefficients that must be used in equation (52) are reported in Appendix. In this way all the quantities are expressed as a function of two variables, $\mathcal{P}$ and T. These functions can be used in the pressure range $10^{-2}\div10^{2}$ atm. Due to the polynomial expression, the extrapolation from recommended range is not possible. On the other hand, the temperature dependence is very accurate in the temperature range 50−60 000 K. In the following, we present analytical expressions for the gas composition (molar fractions), specific entropy, mean molar mass, specific enthalpy, thermal and electric conductivities and viscosity. Relative errors of analytical expressions are always less than 5%. Figure 8 shows the comparison of specific heat at constant pressure for $\mathcal{P}=10^{-2}$, 10^{2} atm and the percentage relative errors, always less than 4%.

Mean molar mass (kg/mol) and gas density (kg/m^3)

$$\overline{M}=c_0-\sum_{j=1}^{6}a_j\sigma_j\left(T\right) \tag{53}$$
$$\rho=\frac{p}{RT}\overline{M}. \tag{54}$$

Specific enthalpy (cal/g)

$$\mathcal{H}=\sum_{j=1}^{2}c_jT^j+\sum_{j=1}^{7}a_j\sigma_j\left(T\right). \tag{55}$$

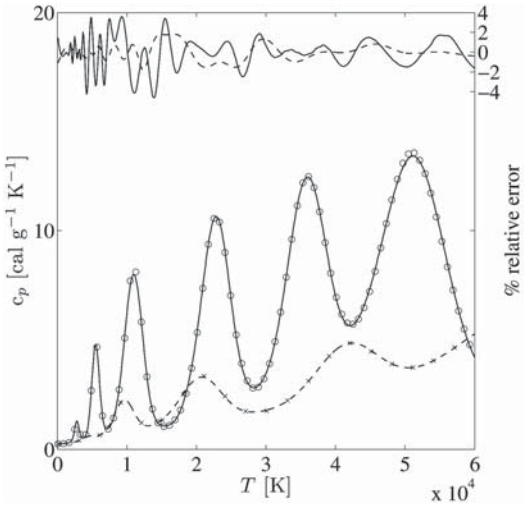

Fig. 8. Comparison of specific heat at constant pressure for $\mathcal{P}=10^{-2}$ atm (full line) and $\mathcal{P}=10^{2}$ atm (dashed line). Values obtained by using the analytical expressions (o, ×) given by equation (56) and correspondent percentage relative errors have been reported.

Specific heat (cal/g/K)

$$c_p=\sum_{j=0}^{1}c_jT^j+\sum_{j=1}^{5}a_j\sigma_j\left(T\right)+\sum_{j=6}^{11}a_j\gamma_j\left(T\right). \tag{56}$$

Specific entropy (cal/g/K)

$$S=\sum_{j=1}^{7}a_j\sigma_j\left(T\right)+\varphi_0\left(T\right). \tag{57}$$

Electric conductivity (S/m)

$$\log\sigma=\xi_0\left(\log\left(T\right)\right)+\sum_{j=1}^{7}a_j\sigma_j\left(T\right). \tag{58}$$

Thermal conductivity (W/K/m)

$$\log\lambda=a_0+\sum_{j=1}^{6}a_j\sigma_j\left(\log\left(T\right)\right)+\sum_{j=7}^{10}a_j\gamma_j\left(\log\left(T\right)\right). \tag{59}$$

Viscosity (Kg/m/s)

$$\log\eta=\log\left[\xi_0\left(T\right)+\sum_{j=1}^{5}a_j\sigma_j\left(T\right)\right]+\sum_{j=6}^{10}a_j\sigma_j\left(T\right). \tag{60}$$

Molar fractions are combinations of sigmoid functions

$$\chi=\max\left[0,\sum_{j=1}^{N}a_j\sigma_j\left(T\right)\right]. \tag{61}$$

Some of the sigmoids are increasing (coefficient a is positive) and some others are decreasing (coefficient a is negative). The sum of the amplitude of the increasing functions are equal to the sum of the amplitudes of decreasing

functions or

$$\sum_i a_i = 0. \tag{62}$$

As a consequence, the amplitude of one of the sigmoids is the linear combination of the amplitude of the others. This role has two exceptions: the species that do not disappear at high temperature (electrons and highly charged atoms) and the species predominant at low temperature (in particular N_2 and O_2), which are the only species which has a coefficient c_0 different from zero.

5 Conclusions

In the paper chemical compositions, thermodynamic and transport properties of air plasma have been calculated in the temperature range 50−60 000 K and for pressure varying from 0.01 to 100 atm. Calculated values have been fitted by analytical functions and fitting coefficients have been reported in Appendix.

For the calculation, use is made of the recent compilation of collision integrals obtained by Capitelli et al. [17]. Comparisons of the present data with literature values at atmospheric pressure show a satisfactory agreement especially with the recent calculations of Murphy [25]. It has been shown that some discrepancies are present especially at high pressure comparing the results obtained with two different cut-off criteria: a constant cut-off and a self-consistent cut-off. Moreover electric conductivity and thermal conductivity depend strongly on the choice of collisions integrals between charged particles. In this paper the method proposed by Mason, which takes into account screened Coulomb potential with a Debye length calculated only from the electron number density, has been considered and large discrepancies respect to the results obtained considering Liboff collision integrals have been observed.

References

1. K.N. Kim, O.H. Rho, C. Park, J. Thermophys. Heat Transf. **14**, 250 (2000)
2. P. Fauchais, M. Vardelle, Pure Appl. Chem. **66**, 1247 (1994)
3. R. Foest, F. Adler, F. Sigeneger, M. Schmidt, Surf. Coat. Technol. **163–164**, 323 (2003)
4. M. Cada, O. Churpita, Z. Hubicka, H. Sichova, L. Jastrabik, Surf. Coat. Technol. **177–178**, 699 (2004)
5. L. Soukup, Z. Hubicka, A. Churpita, M. Cada, P. Pokorny, J. Zemek, P. Jurek, L. Jastrabik, Surf. Coat. Technol. **169–170**, 571 (2003)
6. W.J. Xu, J.C. Fang, Y.S. Lu, J. Mater. Process. Technol. **129**, 152 (2002)
7. P. Sichler, S. Büttgenbach, L. Baars-Hibbe, C. Schrader, K.H. Gericke, Chem. Eng. J. **101**, 465 (2004)
8. N. Barcza, in *Plasma Technology in Metallurgy*, edited by J. Feinman, Iron and Steel Soc. of AIME (1987)
9. P. Fauchais, A. Vardelle, A. Denoirjean, *9th International Conference on Plasma Surface Engineering* (Garmish, Partenkirschen, D, Sept. 1996)
10. G. Colonna, A. D'Angola, Comp. Phys. Comm. **163**, 177 (2004)
11. G. Colonna, Comp. Phys. Comm. **177**, 493 (2007)
12. D.S. Villars, *Western States Section of the Combustion Institute*, edited by G. Bahn, E. Zuckowsky (Butterworths Scientific Publications, Washington D.C., 1960)
13. D.S. Villars, J. Phys. Chem. **60**, 521 (1959)
14. K.S. Drellishak, AEDC-TDB-64-22 (1964)
15. H.R. Griem, Phys. Rev. **128**, 997 (1962)
16. R.S. Devoto, Phys. Fluids **10**, 2105 (1967)
17. M. Capitelli, C. Gorse, S. Longo, D. Giordano, J. Thermophys. Heat Transf. **14**, 259 (2000)
18. R.L. Liboff, Phys. Fluids **2**, 40 (1959)
19. E.A. Mason, R.J. Munn, F.J. Smith, Phys. Fluids **10**, 1827 (1967)
20. H. Hahn, E.A. Mason, F.J. Smith, Phys. Fluids **14**, 278 (1971)
21. M. Capitelli, G. Colonna, C. Gorse, A. D'Angola, Eur. Phys. J. D **11**, 279 (2000)
22. D.L. Landau, E.M. Lifshitz, *Statistical Physics* (Pergamon Press, 1986)
23. E. Asinovsky, A. Kirillin, E. Pakhomov, V. Shabashov, Proc. IEEE **59**, 592 (1971)
24. P.W. Schreiber, A.M. Hunter, K.R. Benedetto, AIAA J. **11**, 2696 (1973)
25. A.B. Murphy, Plasma Chem. Plasma Process. **15**, 279 (1995)
26. C. Hansen, Technical Rep. NASA – TR – R50 (Ames Research Center, Ames, Iowa, 1960)
27. W.E. Nicolet, C.E. Shepard, K.J. Clark, A. Balakrishnan, J.P. Kesserling, K.E. Suchsland, J.J. Reese, Report AEDC-TR-75-47 (1975)
28. J.M. Yos, AVC-RAD (1967)
29. J. Bacri, S. Raffanel, Plasma Chem. Plasma Process. **7**, 53 (1987)
30. J. Bacri, S. Raffanel, Plasma Chem. Plasma Process. **9**, 133 (1989)
31. J.O. Hirschfelder, C.F. Curtiss, R.B. Bird, *Molecular Theory of Gases and Liquids* (Wiley, New York, 1964)
32. S. Chapman, T.G. Cowling, *The Mathematical Theory of Nonuniform Gases* (Cambridge University Press, Cambridge, 1970)
33. D. Giordano, M. Capitelli, G. Colonna, C. Gorse, ESA STR-236 (1994)
34. M. Capitelli, G. Colonna, D. Giordano, L. Marraffa, A. Casavola, P. Minelli, D. Pagano, L.D. Pietanza, F. Taccogna, ESA STR-246 (2005)
35. G. Herzberg, *Molecular Spectra and Molecular Structure: I Diatomic Molecules* (Prentice Hall Inc., New York, 1939)
36. G. Herzberg, *Molecular Spectra and Molecular Structure: II Infrared and Raman Specrta of Polyatomic Molecules* (D. Van Nostrand Co. Inc., New York, 1945)
37. M. Capitelli, Z. Naturforsch. A **29a**, 953 (1974)
38. D. Giordano, M. Capitelli, G. Colonna, C. Gorse, ESA STR-237 (1994)
39. C. Moore, NSRDS-NBS-35 (1971), Vol. 1
40. `http://physics.nist.gov/PhysRefData/ASD1/`
41. H. Margenau, M. Lewis, Rev. Mod. Phys. **31**, 594 (1959)
42. K.S. Drellishak, D.P. Aeschliman, A.B. Cambel, Phys. Fluids **8**, 1590 (1965)
43. J. Hilsenratt, M. Klein, *Tables of Thermodynamic Properties of air in Chemical Equilibrium Including Second Virial Corrections from 1500 K to 15000 K*, AEDC-TR-65-58 (1965)

44. M. Capitelli, E. Ficocelli Varracchio, Rev. Int. Htes Temp. et Refract. **14**, 195 (1977)
45. R.M. Sevast'yanov, R.A. Chernyavskaya, J. Eng. Phys. Thermophys. **51**, 851 (1986)
46. V.B. Leonas, Soviet Physics-Uspekhi **15**, 266 (1973)
47. V.V. Riabov, J. Thermophys. Heat Transf. **10**, 209 (1996)
48. V.P. Glushko, **I**, (VINITI, Moscow, 1971), 332
49. E.W. Mc Daniel, E.A. Mason, *Mobility and diffusion of Ions in Gases* (Wiley, New York, 1973), pp. 344–354
50. J. Stallcop, H. Partridge, E. Levine, J. Thermophys. Heat Transf. **10**, 697 (1996)
51. H. Partridge, J. Stallcop, E. Levine, Chem. Phys. Lett. **184**, 505 (1991)
52. M. Capitelli, R.S. Devoto, Phys. Fluids **16**, 1835 (1967)
53. M. Krauss, D. Neumann, A.C. Wahl, G. Das, W. Zemke, Phys. Rev. A **7**, 69 (1973)
54. Y.N. Belyaev, B.G. Brezhnev, E.M. Erastov, Soviet Physics-JETP **27**, 924 (1968)
55. J.A. Rutherford, D.A. Vroom, J. Chem. Phys. **61**, 2514 (1974)
56. E.I. Duman, A.V. Yevseyev, A.V. Eletski, A.A. Radzig, B.M. Smirnov, *Report Kurchatov Atomic Energy Institute 3532/12* (1982)
57. A.V. Phelps, L.C. Pitchford, University of Colorado, JILA Information Center Rept. 26, boulder, CO, June 1985
58. A.V. Phelps, *Swarm Studies and Inelastic Electron-Molecule collisions*, edited by L.C. Pitchford, B.V. McKoy, A. Chutiyan, S. Traymar (Springer-Verlag, New York, 1987), pp. 127–141
59. N. Chandra, A. Temkin, NASA TN D-8347 (1976)
60. T.W. Shyn, G.R. Caringan, Phys. Rev. A **22**, 923 (1980)
61. D.G. Thomson, J. Phys. B Atom. Mol. Phys. **4**, 468 (1971)
62. L.D. Thomas, R.K. Nesbet, Phys. Rev. A **12**, 2369 (1975)
63. M. Blaha, J. Davis, Phys. Rev. A **12**, 2319 (1975)
64. R.S. Devoto, J. Plasma Phys. **2**, 617 (1968)
65. A.B. Murphy, Plasma Chem. Plasma Proc. **20**, 279 (2000)
66. P. André, W. Bussière, D. Rochette, Plasma Chem. Plasma Proc. **27**, 381 (2007)
67. M.J. Wright, D. Bose, G.E. Palmer, E. Levin, AIAA J. **43**, 2558 (2005)
68. J.N. Butler, R.S. Brokaw, J. Chem. Phys. **26**, 1636 (1956)
69. A. Eucken, Z. Phys. **14**, 324 (1913)
70. D. Bruno, M. Capitelli, C. Catalfamo, A. Laricchiuta, Phys. Plasmas **14**, 072308 (2007)
71. D. Bruno, A. Laricchiuta, M. Capitelli, C. Catalfamo, Phys. Plasmas **14**, 022303 (2007)
72. B. Sourd, P. André, J. Aubreton, M.-F. Elchinger, Plasma Chem. Plasma Process. **27**, 35 (2007)
73. B. Sourd, P. André, J. Aubreton, M.-F. Elchinger, Plasma Chem. Plasma Process. **27**, 225 (2007)
74. A.V. Kosarim, B.M. Smirnov, J. Exp. Theor. Phys. **101**, 611 (2005)
75. A.V. Kosarim, B.M. Smirnov, M. Capitelli, R. Celiberto, A. Laricchiuta, Phys. Rev. A **74**, 1 (2006)
76. A. Eletskii, M. Capitelli, R. Celiberto, A. Laricchiuta, Phys. Rev. A **69**, 1 (2004)
77. R.S. Devoto, Phys. Fluids **9**, 1230 (1966)
78. B. Chervy, A. Gleizes, J. Phys. D: Appl. Phys. **20**, 2557 (1998)
79. M. Capitelli, E. Ficocelli, E. Molinari, Z. Naturforsch. **26a**, 672 (1971)

Appendix A: Fitting coefficients

In this appendix, we report the coefficients (Tabs. 2–27) to obtain analytical expressions of chemical compositions, thermodynamic and transport properties in the temperature range 50–60 000 K and in the pressure range $10^{-2} \div 10^{2}$ atm.

Table 2. Coefficients to calculate molar fraction of N_2 by using $\chi_{N_2}(T) = c_0 - \sum_{j=1}^{2} a_j \sigma_j(T)$.

		α_0	α_1	α_2	α_3	α_4
c_0		0.8	–	–	–	–
	$a_1 = c_0 - a_2$	–	–	–	–	–
σ_1	$\log c_1$	8.110148	4.553237e-2	−8.193725e-4	−2.156896e-4	–
	$\log \Delta_1$	6.561427	1.422222e-1	−7.476314e-4	−8.715905e-4	–
	$\log a_2$	−4.037422e-1	−7.147343e-4	4.492235e-4	9.648313e-5	−1.284083e-8
σ_2	$\log c_2$	8.812799	5.665883e-2	1.293767e-3	–	–
	$\log \Delta_2$	7.016774	1.058804e-1	3.292541e-3	2.267238e-4	–

Table 3. Coefficients to calculate molar fraction of N_2^+ by using $\chi_{N_2^+}(T) = \max\left[0, \sum_{j=1}^{3} a_j \sigma_j(T)\right]$.

		α_0	α_1	α_2	α_3	α_4	α_5
	$\log a_1$	−9.746298	4.199007e-1	3.143417e-3	3.882378e-4	–	–
σ_1	$\log c_1$	8.884490	5.573065e-2	1.616982e-3	6.738352e-5	–	–
	$\log \Delta_1$	6.552069	1.058201e-1	3.989777e-3	1.801416e-4	–	–
	$a_2 = a_3 - a_1$	–	–	–	–	–	–
σ_2	$\log c_2$	9.203463	7.494796e-2	2.541069e-3	7.257196e-5	6.051419e-6	–
	$\log \Delta_2$	7.294752	−1.099569e-3	4.040325e-3	2.717526e-3	−5.081078e-5	−3.474609e-5
	$\log(-a_3)$	−9.992503	4.689265e-1	1.182887e-3	−1.176687e-4	–	–
σ_3	$\log c_3$	9.449201	6.238298e-2	1.564727e-3	5.575073e-5	–	–
	$\log \Delta_3$	7.762006	1.260807e-1	2.223845e-3	−1.231135e-4	–	–

Table 4. Coefficients to calculate molar fraction of N by using $\chi_N(T) = \max\left[0, a_1 \sigma_m(T)\,\sigma_1(T) + \sum_{j=2}^{3} a_j \sigma_j(T)\right]$.

		α_0	α_1	α_2	α_3	α_4
	a_1	8.188731e-1	2.581889e-3	1.395103e-4	–	–
σ_1	$\log c_1$	8.812279	5.474146e-2	1.019131e-3	–	–
	$\log \Delta_1$	7.051737	1.128378e-1	2.407727e-3	−1.247502e-5	–
σ_m	$\log c_m$	8.405373	4.371184e-2	1.893389e-3	1.927737e-4	–
	$\log \Delta_m$	6.923056	1.987863e-1	3.645361e-3	−5.777817e-4	–
	$a_2 = a_3 - a_1$	–	–	–	–	–
σ_2	$\log c_2$	9.516473	6.520807e-2	1.270979e-3	−3.857140e-5	−5.540006e-6
	$\log \Delta_2$	7.949412	1.206502e-1	1.785666e-3	−3.344976e-5	–
	$\log(-a_3)$	−3.552214	4.085111e-1	−2.961084e-2	–	–
σ_3	$\log c_3$	9.864059	3.659617e-2	7.907898e-3	–	–
	$\log \Delta_3$	8.814892	5.421480e-2	1.537056e-3	–	–

Table 5. Coefficients to calculate molar fraction of N^+ by using $\chi_{N^+}(T) = \max\left[0, a_1\sigma_m(T)\,\sigma_1(T) + \sum_{j=2}^{4} a_j\sigma_j(T)\right]$.

		α_0	α_1	α_2	α_3	α_4	α_5
	$\log a_1$	−1.211184	2.634222e-4	2.560470e-3	–	–	–
σ_1	$\log c_1$	9.494309	5.588021e-2	2.479295e-3	5.228102e-4	5.047984e-5	−1.606423e-6
	$\log \Delta_1$	8.228344	2.288911e-1	−7.989931e-4	−1.145501e-3	–	–
σ_m	$\log c_m$	9.276675	8.451791e-2	−7.509912e-3	1.762683e-3	−2.856325e-4	3.392616e-5
	$\log \Delta_m$	7.931270	−4.388112e-2	2.643605e-2	−1.501361e-3	−2.178943e-4	2.476492e-5
	$\log a_2$	−2.230927	2.047906e-2	−2.220684e-3	–	–	–
σ_2	$\log c_2$	9.511003	8.651691e-2	−5.130145e-5	−2.847046e-4	–	–
	$\log \Delta_2$	7.645166	8.574186e-2	2.708947e-4	6.210369e-4	–	–
	$a_3 = a_4 - a_2 - a_1$	–	–	–	–	–	–
σ_3	$\log c_3$	1.037880e+1	6.497169e-2	3.027193e-3	1.559114e-4	−2.230902e-7	3.440378e-6
	$\log \Delta_3$	8.810742	1.305064e-1	−1.083168e-3	4.025862e-5	1.348428e-4	−2.273123e-5
	$\log(-a_4)$	−1.200529	−3.074481e-2	4.780888e-3	8.341989e-4	6.160353e-6	−2.708386e-6
σ_4	$\log c_4$	1.025494e+1	6.494578e-2	1.277401e-3	–	–	–
	$\log \Delta_4$	8.187912	1.182600e-1	6.307194e-3	2.948945e-4	1.136590e-6	–

		α_6	α_7
	$\log a_1$	–	–
σ_1	$\log c_1$	−8.671283e-7	−5.919943e-8
	$\log \Delta_1$	–	–
σ_m	$\log c_m$	−5.010435e-6	3.875277e-7

Table 6. Coefficients to calculate molar fraction of N^{++} by using $\chi_{N^{++}}(T) = \max\left[0, a_1\sigma_m(T)\,\sigma_1(T) + \sum_{j=2}^{3} a_j\sigma_j(T)\right]$.

		α_0	α_1	α_2	α_3	α_4
	$\log a_1$	−1.320561	4.613513e-3	1.563146e-3	9.805924e-5	–
σ_1	$\log c_1$	1.018105e+1	6.182886e-2	4.542717e-4	1.665348e-4	−1.688929e-5
	$\log \Delta_1$	8.328213	7.134338e-2	8.440573e-3	−1.913632e-4	–
σ_m	$\log c_m$	1.020635e+1	6.787015e-2	2.930559e-3	−2.387278e-5	−1.580874e-5
	$\log \Delta_m$	8.637046	1.730873e-1	−2.312739e-3	−1.253255e-4	6.870714e-5
	$a_2 = a_3 - a_1$	–	–	–	–	–
σ_2	$\log c_2$	1.071778e+1	6.267958e-2	1.384143e-3	1.803319e-5	–
	$\log \Delta_2$	8.558877	1.280075e-1	7.408166e-3	−6.068102e-5	−3.499092e-5
	$\log(-a_3)$	−2.441955	1.600937e-2	−1.796504e-2	4.445771e-5	–
σ_3	$\log c_3$	1.081164e+1	6.929471e-2	3.005312e-3	5.422861e-5	–
	$\log \Delta_3$	9.008121	1.059058e-1	3.835047e-3	−5.778232e-4	–

Table 7. Coefficients to calculate molar fraction of N^{+++} by using $\chi_{N^{+++}}(T) = \max\left[0, a_1\sigma_m(T)\,\sigma_1(T) - a_1\sigma_2(T)\right]$.

		α_0	α_1	α_2	α_3
	$\log a_1$	−1.339800	1.954622e-2	−3.939015e-3	−4.170049e-4
σ_1	$\log c_1$	1.070665e+1	6.722548e-2	6.769799e-5	4.111595e-5
	$\log \Delta_1$	9.340050	5.929963e-2	1.505109e-3	2.034159e-4
σ_m	$\log c_m$	1.066404e+1	5.711793e-2	1.063676e-3	−1.137507e-6
	$\log \Delta_m$	8.726521	1.521811e-1	2.430293e-3	−4.716643e-4
σ_2	$\log c_2$	1.105085e+1	5.890335e-2	1.918852e-3	9.521033e-5
	$\log \Delta_2$	9.258763	1.273121e-1	−6.021997e-4	−2.540618e-4

Table 8. Coefficients to calculate molar fraction of N^{++++} by using $\chi_{N^{++++}}(T) = \max\left[0, a_1\sigma_m(T)\,\sigma_1(T) + \sum_{j=2}^{3} a_j\sigma_j(T)\right]$.

		α_0	α_1	α_2	α_3	α_4
	$\log a_1$	−1.849635	−4.491118e-3	−3.702617e-4	–	–
σ_1	$\log c_1$	1.100960e+1	7.368509e-2	1.075589e-3	–	–
	$\log \Delta_1$	9.329126	7.704932e-2	2.666225e-3	–	–
σ_m	$\log c_m$	1.100986e+1	4.882927e-2	3.853047e-4	−1.475967e-6	–
	$\log \Delta_m$	9.006971	1.074664e-1	−1.472426e-3	−2.722012e-4	–
	$a_2 = a_3 - a_1$	–	–	–	–	–
σ_2	$\log c_2$	1.206372e+1	−1.734608e-3	−1.447988e-2	1.590266e-3	–
	$\log \Delta_2$	1.019997e+1	−1.423777e-1	−4.095877e-2	2.180861e-3	2.368183e-4
	$\log(-a_3)$	−6.074622e-1	6.073274e-1	9.963043e-2	5.415504e-3	–
σ_3	$\log c_3$	1.280436e+1	−1.896326e-1	2.801196e-2	–	–
	$\log \Delta_3$	1.103058e+1	−2.553162e-1	2.330651e-2	–	–

Table 9. Coefficients to calculate molar fraction of O_2 by using $\chi_{O_2}(T) = c_0 - \sum_{j=1}^{2} a_j\sigma_j(T)$.

		α_0	α_1	α_2	α_3	α_4	α_5
c_0		0.2	–	–	–	–	–
	$a_1 = c_0 - a_2$	–	–	–	–	–	–
σ_1	$\log c_1$	7.851965	−4.971670e-2	−1.438515e-2	−8.639710e-4	–	–
	$\log \Delta_1$	6.500431	7.318423e-2	−2.704126e-3	−2.824658e-4	–	–
	$\log a_2$	−1.685730	3.728595e-2	−5.172240e-3	2.021941e-4	6.195083e-5	−5.999263e-6
σ_2	$\log c_2$	8.148167	4.575379e-2	1.841872e-4	–	–	–
	$\log \Delta_2$	6.459154	1.486515e-1	5.919587e-3	−3.159509e-5	−4.048213e-5	–

Table 10. Coefficients to calculate molar fraction of O_2^+ by using $\chi_{O_2^+}(T) = \max\left[0, \sum_{j=1}^{4} a_j\sigma_j(T)\right]$.

		α_0	α_1	α_2	α_3	α_4
	$\log a_1$	−1.373444e+1	6.627381e-1	−1.950471e-2	7.469315e-4	1.358278e-4
σ_1	$\log c_1$	8.794853	4.659480e-2	5.610403e-4	1.044006e-4	−1.835079e-5
	$\log \Delta_1$	7.268996	9.440745e-2	−2.146537e-3	4.167152e-5	3.077941e-5
	$\log a_2$	−1.419853e+1	4.889623e-1	−6.123742e-3	5.940913e-4	9.783232e-5
σ_2	$\log c_2$	8.991604	5.142449e-2	1.298498e-3	4.051458e-4	1.170299e-5
	$\log \Delta_2$	7.456563	1.277214e-1	8.479742e-3	8.341173e-4	−1.597360e-4
	$a_3 = a_4 - a_2 - a_1$	–	–	–	–	–
σ_3	$\log c_3$	9.563817	7.340431e-2	7.915772e-4	−1.592330e-4	−1.027704e-5
	$\log \Delta_3$	7.834428	1.245447e-1	4.949361e-3	3.875066e-5	−2.966365e-5
	$\log(-a_4)$	−1.342851e+1	6.025406e-1	−1.482459e-2	1.461126e-4	1.408990e-4
σ_4	$\log c_4$	8.900254	3.563862e-2	1.399785e-3	1.003372e-4	−3.618984e-5
	$\log \Delta_4$	7.450971	9.288765e-2	−1.491663e-3	7.510663e-4	−9.458429e-5

Table 11. Coefficients to calculate molar fraction of O_2^- by using $\chi_{O_2^-}(T) = \max\left[0, \sum_{j=1}^{4} a_j \sigma_j(T)\right]$.

		α_0	α_1	α_2	α_3	α_4
	$\log a_1$	−2.009128e+1	1.218472	−1.023713e-2	−3.693487e-4	–
σ_1	$\log c_1$	8.151744	5.269669e-2	1.328087e-3	9.918314e-5	6.931618e-6
	$\log \Delta_1$	6.140093	1.051897e-1	2.939827e-3	1.422812e-4	–
	$a_2 = a_4 + a_3 - a_1$	–	–	–	–	–
σ_2	$\log c_2$	8.327753	6.884887e-2	2.843931e-3	1.083879e-4	–
	$\log \Delta_2$	6.644117	1.374513e-1	4.095263e-3	8.402722e-5	−1.242256e-5
	$\log(-a_3)$	−2.169571e+1	1.231117	1.792651e-3	2.558252e-4	−1.732401e-4
σ_3	$\log c_3$	8.601320	7.342289e-2	−9.411900e-4	−1.339663e-4	3.126379e-5
	$\log \Delta_3$	6.985630	8.256947e-2	9.999196e-3	−2.953396e-5	−1.526330e-4
	$\log(-a_4)$	−2.472870e+1	1.526884	1.203852e-3	1.430794e-4	–
σ_4	$\log c_4$	9.428115	5.014640e-2	−3.340382e-4	7.998702e-6	–
	$\log \Delta_4$	7.530896	1.558330e-1	4.905502e-3	−8.411242e-4	–

		α_5	α_6	α_7
σ_2	$\log \Delta_2$	−7.990825e-6	8.075101e-7	2.001120e-7
σ_3	$\log(-a_3)$	8.498995e-6	1.264359e-6	–

Table 12. Coefficients to calculate molar fraction of O by using $\chi_O(T) = \max\left[0, a_1 \sigma_m(T)\sigma_1(T) + \sum_{j=2}^{4} a_j \sigma_j(T)\right]$.

		α_0	α_1	α_2	α_3	α_4	α_5
	$\log a_1$	−1.139281	−1.050647e-2	−1.022007e-3	−4.830320e-5	−3.531305e-6	−2.296630e-7
σ_1	$\log c_1$	8.145639	5.431612e-2	2.023998e-3	1.003745e-4	–	–
	$\log \Delta_1$	6.576786	1.491330e-1	3.724868e-3	−1.382563e-4	1.947915e-6	1.082756e-6
σ_m	$\log c_m$	7.940783	6.741169e-2	−2.087042e-3	3.972481e-4	−3.481686e-5	1.485858e-6
	$\log \Delta_m$	6.664764	4.575484e-2	4.557480e-3	–	–	–
	$\log(-a_2)$	−4.979500	2.665257e-1	1.458327e-2	−2.533456e-3	−3.704428e-4	2.339924e-5
σ_2	$\log c_2$	9.811744	7.436247e-2	−1.239267e-4	6.132060e-4	–	–
	$\log \Delta_2$	9.044853	5.997097e-3	4.532508e-4	6.756744e-4	–	–
	$a_3 = a_4 + a_2 - a_1$	–	–	–	–	–	–
σ_3	$\log c_3$	8.819734	5.805213e-2	1.501067e-3	2.511693e-5	–	–
	$\log \Delta_3$	6.918048	9.326905e-2	2.506390e-3	1.395474e-4	–	–
	$\log(-a_4)$	−1.615594	−5.157778e-3	−1.550658e-3	−1.264223e-4	2.343404e-5	3.184705e-6
σ_4	$\log c_4$	9.554277	6.746571e-2	8.910292e-4	−4.496226e-5	–	–
	$\log \Delta_4$	8.033301	1.233674e-1	1.651217e-3	−3.811131e-5	–	–

Table 13. Coefficients to calculate molar fraction of O^- by using $\chi_{O^-}(T) = \max\left[0, \sum_{j=1}^{3} a_j \sigma_j(T)\right]$.

		α_0	α_1	α_2	α_3	α_4
	$\log a_1$	−1.492297e+1	9.064321e-1	−8.724265e-3	−2.165125e-4	1.166368e-4
σ_1	$\log c_1$	8.415326	5.157258e-2	2.024706e-3	1.312425e-4	1.315036e-5
	$\log \Delta_1$	6.462668	6.272626e-2	−6.193918e-3	6.376014e-4	2.245471e-4
	$\log a_2$	−1.175041e+1	7.618857e-1	1.501595e-3	1.781504e-4	9.215991e-6
σ_2	$\log c_2$	9.270258	5.316281e-2	1.482070e-3	−5.476676e-5	−9.733849e-6
	$\log \Delta_2$	7.724023	9.838486e-2	4.215920e-3	−6.990084e-5	−3.230965e-5
	$a_3 = -a_1 - a_2$	–	–	–	–	–
σ_3	$\log c_3$	9.598507	6.569448e-2	5.303147e-4	−9.613381e-5	−7.330576e-6
	$\log \Delta_3$	7.809041	1.423877e-1	4.366188e-3	−8.184536e-5	−1.524608e-5

Table 14. Coefficients to calculate molar fraction of O^+ by using $\chi_{O^+}(T) = \max\left[0, a_1\sigma_m(T)\,\sigma_1(T) + \sum_{j=2}^{3} a_j\sigma_j(T)\right]$.

		α_0	α_1	α_2	α_3	α_4
	$\log a_1$	−2.319093	−7.610174e-3	−1.953269e-3	−3.002482e-4	−1.751192e-5
σ_1	$\log c_1$	9.588569	6.997026e-2	9.769379e-4	−6.246775e-5	−4.877947e-6
	$\log \Delta_1$	8.044970	1.175891e-1	1.645336e-3	−9.489377e-5	−9.694619e-6
σ_m	$\log c_m$	9.115221	6.168847e-2	2.270858e-3	1.412631e-4	–
	$\log \Delta_m$	7.651684	1.477558e-1	−1.967294e-3	−9.075769e-4	–
	$a_2 = a_3 - a_1$	–	–	–	–	–
σ_2	$\log c_2$	1.020364e+1	6.299762e-2	−1.091887e-3	3.702998e-5	–
	$\log \Delta_2$	8.680331	1.325526e-1	2.754338e-3	−7.964755e-5	–
	$\log(-a_3)$	−1.436906	2.872384e-1	2.978317e-2	1.769679e-4	−9.414001e-5
σ_3	$\log c_3$	1.027215e+1	4.672465e-2	1.597850e-4	9.311678e-6	–
	$\log \Delta_3$	8.696369	1.339624e-1	1.995427e-3	−3.323281e-5	–

Table 15. Coefficients to calculate molar fraction of O^{++} by using $\chi_{O^{++}}(T) = \max\left[0, a_1\sigma_m(T)\,\sigma_1(T) + \sum_{j=2}^{3} a_j\sigma_j(T)\right]$.

		α_0	α_1	α_2	α_3
	a_1	7.063013e-2	−5.187789e-4	−9.288238e-6	–
σ_1	$\log c_1$	1.029003e+1	4.517420e-2	−1.618224e-5	2.245678e-4
	$\log \Delta_1$	8.449025	1.233942e-1	−3.128794e-3	−5.456369e-4
σ_m	$\log c_m$	1.029386e+1	8.048612e-2	−4.497818e-4	3.852087e-5
	$\log \Delta_m$	8.843594	4.195145e-2	1.187095e-2	1.964457e-4
	$a_2 = a_3 - a_1$	–	–	–	–
σ_2	$\log c_2$	1.082680e+1	7.388982e-2	9.267668e-4	–
	$\log \Delta_2$	9.267200	5.532633e-2	2.362320e-3	6.299569e-4
	$\log(-a_3)$	−2.991458	−5.757422e-2	−3.835760e-3	–
σ_3	$\log c_3$	1.078471e+1	5.999115e-2	1.044468e-3	–
	$\log \Delta_3$	8.785646	9.165132e-2	9.925663e-4	–

		α_4	α_5	α_6
σ_1	$\log c_1$	3.130833e-5	−2.423868e-6	−3.903368e-7
	$\log \Delta_1$	5.445584e-5	6.520078e-6	–
σ_m	$\log \Delta_m$	−4.989937e-5	−9.711143e-7	–
σ_2	$\log \Delta_2$	1.122230e-5	−2.869166e-6	−4.451869e-7

Table 16. Coefficients to calculate molar fraction of O^{+++} by using $\chi_{O^{+++}}(T) = \max[0, a_1\sigma_m(T)\,\sigma_1(T) + a_2\sigma_2(T)]$.

		α_0	α_1	α_2	α_3	α_4	α_5
	$\log a_1$	−2.760009	3.495500e-3	−5.357864e-3	−2.144466e-4	9.251860e-6	−9.005345e-7
σ_1	$\log c_1$	1.074207e+1	5.260080e-2	4.936255e-4	−4.405321e-5	−3.025027e-6	−5.425422e-7
	$\log \Delta_1$	8.835975	1.411710e-1	2.773994e-3	−6.211959e-4	3.813517e-6	1.323357e-5
σ_m	$\log c_m$	1.077506e+1	6.587529e-2	2.491665e-4	1.077355e-4	–	–
	$\log \Delta_m$	9.367809	3.868631e-2	−7.976461e-4	6.108727e-4	–	–
	$a_2 = -a_1$	–	–	–	–	–	–
σ_2	$\log c_2$	1.111558e+1	5.973321e-2	2.038965e-3	9.054082e-5	–	–
	$\log \Delta_2$	9.317898	1.146590e-1	−4.219919e-4	−1.986513e-4	−9.501572e-6	–

		α_6	α_7
σ_1	$\log \Delta_1$	−1.119305e-6	−3.062376e-7

Table 17. Coefficients to calculate molar fraction of O^{++++} by using $\chi_{O^{++++}}(T) = \max\left[0, a_1\sigma_m(T)\,\sigma_1(T) + \sum_{j=2}^{3} a_j\sigma_j(T)\right]$.

		α_0	α_1	α_2	α_3	α_4	α_5
	$\log a_1$	−3.273424	−9.222532e-3	−2.546540e-3	−6.142466e-4	−6.803461e-5	−1.480622e-6
σ_1	$\log c_1$	1.114079e+1	6.128099e-2	1.305781e-3	−4.745385e-5	−1.294845e-5	−6.416314e-7
	$\log \Delta_1$	9.124558	1.015232e-1	−1.452067e-3	−4.363441e-4	−9.737843e-6	1.643326e-6
σ_m	$\log c_m$	1.097387e+1	5.385207e-2	3.454294e-5	−9.334055e-5	–	–
	$\log \Delta_m$	9.008289	5.266326e-2	−2.558320e-4	3.532844e-5	–	–
	$a_2 = a_3 - a_1$	–	–	–	–	–	–
σ_2	$\log c_2$	1.133963e+1	5.445065e-2	−3.976441e-4	1.251159e-4	–	–
	$\log \Delta_2$	9.165912	3.362575e-2	1.118630e-3	−3.084012e-4	−7.665827e-5	–
	$\log(-a_3)$	−3.227410	−4.108171e-3	−6.841752e-4	−3.928651e-5	–	–
σ_3	$\log c_3$	1.473199e+1	−3.158041e-1	−3.070674e-2	6.776443e-3	–	–
	$\log \Delta_3$	1.306288e+1	−3.228563e-1	−3.275522e-2	6.750116e-3	–	–

Table 18. Coefficients to calculate molar fraction of NO by using $\chi_{NO}(T) = \max\left[0, \sum_{j=1}^{3} a_j\sigma_j(T)\right]$.

		α_0	α_1	α_2	α_3	α_4
	$\log a_1$	−2.397641	9.644207e-2	–	–	–
σ_1	$\log c_1$	7.942600	2.917164e-2	6.775381e-4	2.209082e-5	–
	$\log \Delta_1$	6.780323	6.029139e-2	4.276063e-4	–	–
	$a_2 = a_3 - a_1$	–	–	–	–	–
σ_2	$\log c_2$	8.274503	6.655621e-2	2.214534e-3	3.856329e-5	–
	$\log \Delta_2$	6.495225	7.930874e-2	−1.952605e-3	−7.384374e-4	−5.231985e-5
	$\log(-a_3)$	−2.923272	1.671984e-1	–	–	–
σ_3	$\log c_3$	8.364477	7.365241e-2	2.771836e-3	−5.013391e-6	−5.293616e-6
	$\log \Delta_3$	7.549495	9.399569e-2	–	–	–

Table 19. Coefficients to calculate molar fraction of NO^+ by using $\chi_{NO^+}(T) = \max\left[0, \sum_{j=1}^{4} a_j\sigma_j(T)\right]$.

		α_0	α_1	α_2	α_3	α_4	α_5
	$\log a_1$	−7.135266	4.617651e-2	−7.097386e-4	–	–	–
σ_1	$\log c_1$	8.740893	4.144123e-2	3.456197e-4	–	–	–
	$\log \Delta_1$	6.996599	6.789593e-2	1.320085e-3	2.143434e-5	6.597691e-6	1.625852e-7
	$\log a_2$	−8.753925	1.392942e-1	1.317873e-2	–	–	–
σ_2	$\log c_2$	8.817743	4.865084e-2	7.358462e-4	–	–	–
	$\log \Delta_2$	6.260938	9.417073e-2	7.841151e-3	–	–	–
	$a_3 = a_4 - a_2 - a_1$	–	–	–	–	–	–
σ_3	$\log c_3$	8.899564	6.228872e-2	1.910295e-3	5.292903e-5	–	–
	$\log \Delta_3$	7.246371	1.012940e-1	4.389279e-3	−2.344414e-5	−1.533963e-5	–
	$\log(-a_4)$	−8.772596	1.382471e-1	−1.513718e-3	1.822779e-3	5.774867e-5	–
σ_4	$\log c_4$	9.221935	8.005371e-2	3.728793e-3	−1.235847e-4	−6.058282e-6	–
	$\log \Delta_4$	7.940040	1.021609e-1	5.411563e-3	1.592304e-4	−7.583651e-5	–

Table 20. Coefficients to calculate molar fraction of e^- by using $\chi_{e^-}(T) = \max\left[0, a_1\sigma_m(T)\,\sigma_1(T) + \sum_{j=2}^{6} a_j\sigma_j(T)\right]$.

		α_0	α_1	α_2	α_3	α_4	α_5
	$\log a_1$	−3.932487e-1	7.116035e-4	4.083493e-4	3.307562e-4	2.215248e-5	−4.020145e-6
σ_1	$\log c_1$	9.514823	6.426626e-2	3.538392e-4	−1.093881e-4	–	–
	$\log \Delta_1$	7.931006	1.174176e-1	−5.369256e-4	−1.640676e-4	2.876393e-5	–
σ_m	$\log c_m$	6.343867	1.473478	−2.628976e-1	2.653667e-2	−1.170989e-3	–
	$\log \Delta_m$	1.029159e+1	3.502366e-2	−1.043994e-2	−7.498040e-4	1.464646e-4	1.031691e-5
	$\log a_2$	−1.599518	−3.681243e-2	−1.499672e-2	−4.875898e-3	−9.278204e-5	8.792226e-5
σ_2	$\log c_2$	1.025313e+1	6.613035e-2	2.106960e-3	1.249059e-4	−3.254728e-6	−1.073094e-6
	$\log \Delta_2$	8.461864	1.033435e-1	−6.800325e-3	−2.171111e-3	8.042855e-5	3.126866e-5
	$\log a_3$	−3.031217	−1.236964e-2	4.999807e-3	4.130827e-4	−5.879976e-5	−5.643378e-6
σ_3	$\log c_3$	1.074247e+1	6.026184e-2	6.834881e-4	1.412968e-6	–	–
	$\log \Delta_3$	8.457103	1.570495e-1	2.577271e-2	−4.699755e-4	−7.340190e-4	−1.521958e-6
	$\log a_4$	−3.096101	5.690833e-2	1.063005e-2	8.066239e-4	–	–
σ_4	$\log c_4$	1.106632e+1	5.734452e-2	1.326880e-3	4.870977e-5	–	–
	$\log \Delta_4$	9.134358	1.817063e-1	8.463508e-3	–	–	–
	$a_5 = a_6 - a_2 - a_1$	–	–	–	–	–	–
σ_5	$\log c_5$	1.009244e+1	5.691765e-2	2.642057e-3	3.297719e-5	–	–
	$\log \Delta_5$	9.041428	9.809302e-2	1.899235e-3	−1.329754e-4	−2.357106e-5	–
	$\log(-a_6)$	−3.465436e-1	−2.831472e-3	−1.021467e-3	−7.753035e-5	–	–
σ_6	$\log c_6$	1.219498e+2	−3.565001	7.046916e-1	3.062083e-1	−2.940975e-2	–
	$\log \Delta_6$	1.163952e+2	−3.232407	6.981116e-1	2.997466e-1	−2.749064e-2	–

		α_6	α_7
σ_m	$\log \Delta_m$	−3.878009e-7	–
	$\log a_2$	1.273088e-5	–
σ_2	$\log c_2$	−4.149968e-7	−4.918145e-8
	$\log \Delta_2$	3.548083e-6	1.732832e-7
σ_3	$\log a_3$	−2.118479e-7	−8.835667e-8
	$\log \Delta_3$	7.337098e-6	−1.937258e-8

Table 21. Coefficients to calculate mean molar mass according to (53).

		α_0	α_1	α_2	α_3	α_4
c_0		0.028811	–	–	–	–
	$\log a_1$	−5.452539	−2.762076e-2	−3.327630e-3	−2.453118e-4	−6.332107e-6
σ_1	$\log c_1$	8.170734	5.708244e-2	1.293374e-3	–	–
	$\log \Delta_1$	6.380594	1.046470e-1	8.553860e-4	−1.572857e-4	–
	$\log a_2$	−4.595514	1.328152e-2	9.294096e-4	−8.243998e-5	−9.490079e-6
σ_2	$\log c_2$	8.805680	5.468057e-2	1.121881e-3	–	–
	$\log \Delta_2$	7.080690	1.142540e-1	6.869247e-4	−2.257365e-4	–
	$\log a_3$	−4.971377	−1.668833e-2	−2.409638e-3	−2.840529e-4	−2.934495e-5
σ_3	$\log c_3$	9.525862	6.639994e-2	7.836529e-4	−2.447910e-4	−2.415297e-5
	$\log \Delta_3$	7.888211	9.954169e-2	−1.327510e-4	−2.926560e-4	−4.717532e-5
	$\log a_4$	−6.720756	7.203127e-2	6.766486e-3	−1.019894e-3	9.196578e-5
σ_4	$\log c_4$	1.055726e+1	8.397717e-3	9.849480e-4	3.539965e-4	−4.236150e-5
	$\log \Delta_4$	8.707609	3.713173e-2	−1.670186e-2	−5.094908e-4	4.248200e-4
	$\log a_5$	−6.218117	−7.145834e-2	6.529894e-4	1.599394e-3	1.981881e-5
σ_5	$\log c_5$	1.020784e+1	2.553473e-2	−3.549988e-3	–	–
	$\log \Delta_5$	8.422438	1.125955e-1	−3.204629e-3	−1.655103e-3	−2.051312e-4
	$\log a_6$	−6.611171	8.990124e-2	−5.418532e-3	–	–
σ_6	$\log c_6$	1.096136e+1	2.887564e-2	−3.621097e-4	–	–
	$\log \Delta_6$	9.253817	1.341329e-2	−6.004835e-3	1.860800e-3	−1.229602e-4

Table 22. Coefficients to calculate specific enthalpy according to (55).

		α_0	α_1	α_2	α_3	α_4	α_5
c_1		2.350912e-1	−1.120236e-3	−2.508755e-5	–	–	–
c_2		1.542966e-5	6.556647e-7	–	–	–	–
	log a_1	6.587335	−6.112145e-2	−9.108114e-3	−9.569561e-4	−1.128838e-4	−8.757988e-6
σ_1	log c_1	8.164839	5.283021e-2	4.741812e-4	−1.276598e-4	−9.877950e-6	–
	log Δ_1	6.513247	1.040239e-1	−8.104042e-4	−2.991537e-4	4.348437e-5	6.258153e-6
	log a_2	8.740885	3.050736e-3	1.599171e-3	−2.859059e-4	−5.371695e-5	–
σ_2	log c_2	8.856133	5.964702e-2	1.745638e-3	2.343688e-5	−3.102821e-6	–
	log Δ_2	6.981907	1.119408e-1	4.185626e-3	−2.499247e-4	−5.209456e-5	–
	log a_3	1.014496e+1	−1.833015e-2	−4.265166e-3	−8.321612e-4	−6.481810e-5	–
σ_3	log c_3	9.593196	7.089945e-2	1.640521e-3	−1.055407e-4	−1.510653e-5	–
	log Δ_3	7.910995	1.006930e-1	−1.608832e-3	−2.526731e-4	–	–
	log a_4	1.082665e+1	−4.777223e-2	−4.682547e-3	–	–	–
σ_4	log c_4	1.030572e+1	6.607308e-2	1.512694e-3	−5.009486e-5	−5.192881e-6	1.116840e-6
	log Δ_4	8.320951	7.474585e-2	1.789257e-3	5.273341e-4	3.755570e-5	3.425485e-6
	log a_5	1.145937e+1	5.122940e-4	−8.805300e-3	−1.193042e-3	–	–
σ_5	log c_5	1.076031e+1	6.404003e-2	9.621465e-4	−1.883920e-5	–	–
	log Δ_5	8.846750	1.307197e-1	−2.943134e-4	−6.425060e-4	–	–
	log a_6	1.172458e+1	−5.461477e-2	3.413385e-3	7.407737e-4	−1.644220e-4	−1.878043e-5
σ_6	log c_6	1.109244e+1	6.026294e-2	1.125935e-3	−2.170126e-5	−3.141895e-6	–
	log Δ_6	8.942747	8.687938e-2	1.554323e-2	3.584506e-5	−2.447405e-4	–
	log a_7	−1.011841e+1	−2.295953e+1	−1.220667e+1	−3.504472	−4.373233e-1	1.127311e-2
σ_7	log c_7	1.314544e+1	2.079129	9.992304e-1	2.223931e-1	1.963954e-2	−1.622592e-4
	log Δ_7	−1.743314	−1.807206e+1	−1.393980e+1	−5.232064	−7.607736e-1	8.529592e-2

		α_6	α_7	α_8	α_9
	log a_7	6.598926e-3	−2.119755e-4	−1.369506e-4	−8.311253e-6
σ_7	log c_7	−1.094608e-5	2.304744e-5	1.817656e-6	–
	log Δ_7	4.967101e-2	7.733746e-3	5.507513e-4	1.527569e-5

Table 23. Coefficients to calculate specific heat according to (56).

		α_0	α_1	α_2	α_3	α_4
c_0		4.303513e-3	6.487052e-2	−6.616517e-3	2.391262e-4	–
c_1		−2.472201e-5	1.865503e-5	−1.298963e-6	–	–
	log a_1	−3.497916e-1	−2.900058e-1	−3.839544e-2	−6.284876e-3	−4.130292e-4
σ_1	log c_1	1.008338e+1	8.730410e-2	8.590102e-3	5.892083e-4	–
	log Δ_1	8.043134	3.294414e-1	4.681080e-2	−1.509745e-3	−4.534410e-4
	log a_2	−2.305816	9.286290e-2	−1.095463e-2	−1.929857e-3	−2.358095e-4
σ_2	log c_2	7.803107	6.576559e-2	1.214098e-4	−2.773380e-4	–
	log Δ_2	6.212416	1.085758e-1	−1.459860e-2	4.297049e-4	–
	log a_3	1.885717e+1	1.564732e+1	3.946648	2.094257e-1	−4.423704e-2
σ_3	log c_3	1.174382e+1	1.351866e-1	−5.421755e-2	−1.623227e-2	7.438041e-4
	log Δ_3	6.596434	−5.025506	−3.238969	−6.901133e-1	−1.855573e-2
	log a_4	9.844680e-1	−2.553591e-1	−8.898889e-3	1.493946e-3	6.005988e-5
σ_4	log c_4	1.052223e+1	8.741211e-3	−2.198211e-4	–	–
	log Δ_4	9.241400	−6.373646e-2	−7.339952e-3	5.024652e-4	–
	log a_5	4.664598e-1	−2.233574e-1	−1.441672e-2	−1.177062e-3	−6.026800e-5
σ_5	log c_5	8.854075	5.131262e-2	1.507223e-3	3.158892e-4	–
	log Δ_5	8.973554	1.209818e-2	2.753489e-3	2.401117e-4	–

		α_5	α_6
	log a_3	−5.854376e-3	−1.750164e-4
σ_3	log c_3	4.977237e-4	3.456374e-5
	log Δ_3	8.925939e-3	7.161553e-4

		α_0	α_1	α_2	α_3	α_4
	$\log a_6$	−8.639771e-1	−2.135237e-1	−1.735545e-2	−1.885139e-3	−1.226041e-4
γ_6	$\log c_6$	8.164620	5.272624e-2	5.356645e-4	−4.303413e-5	–
	$\log \Delta_6$	6.414342	7.141268e-2	−3.184188e-3	−3.896052e-4	–
	$\log a_7$	9.596448e-1	−1.130686e-1	−2.461674e-3	4.743607e-5	–
γ_7	$\log c_7$	8.857074	5.974192e-2	1.621499e-3	2.811880e-5	–
	$\log \Delta_7$	7.031326	9.966653e-2	2.637695e-3	−3.740228e-5	–
	$\log a_8$	1.431534	−1.255579e-1	−5.407784e-3	−4.894608e-4	–
γ_8	$\log c_8$	9.598608	7.030841e-2	9.720862e-4	−8.467979e-5	–
	$\log \Delta_8$	7.915774	9.011657e-2	−7.629395e-4	−1.579088e-4	–
	$\log a_9$	1.658985	−1.098660e-1	−7.382403e-3	−1.597338e-3	−1.259823e-4
γ_9	$\log c_9$	1.030698e+1	6.396773e-2	1.387554e-3	5.277379e-5	–
	$\log \Delta_9$	8.306511	8.714253e-2	6.812322e-4	–	–
	$\log a_{10}$	1.638978	−1.238859e-1	−3.036868e-3	−1.130285e-3	−1.070291e-4
γ_{10}	$\log c_{10}$	1.076627e+1	6.602355e-2	1.098331e-3	−2.395208e-5	–
	$\log \Delta_{10}$	8.764870	1.276501e-1	−5.083689e-4	−7.452322e-4	2.885332e-5
	$\log a_{11}$	1.933029	−1.248750e-1	−1.646256e-2	5.253210e-4	3.143929e-4
γ_{11}	$\log c_{11}$	1.109308e+1	5.876202e-2	1.243864e-3	3.958414e-5	–
	$\log \Delta_{11}$	8.959570	1.014329e-1	1.073510e-2	−1.155143e-3	−2.731432e-4

Table 24. Coefficients to calculate specific entropy according to (57).

		α_0	α_1	α_2	α_3
φ_0	a_0	7.247773e-1	−5.579293e-2	1.246960e-3	–
	$\log w_0$	−1.949369	4.114017e-2	−1.494867e-4	–
	a_1	2.181324e-1	−2.219875e-2	−3.107110e-4	–
σ_1	$\log c_1$	8.148014	5.310698e-2	1.031964e-3	–
	$\log \Delta_1$	6.487571	1.023051e-1	2.174761e-3	–
	a_2	9.599015e-1	−5.505086e-2	1.666018e-5	–
σ_2	$\log c_2$	8.839993	5.776858e-2	1.370456e-3	–
	$\log \Delta_2$	7.037019	1.068246e-1	2.382441e-3	–
	$\log a_3$	6.970847e-1	−6.594736e-2	−2.375941e-3	−6.719048e-5
σ_3	$\log c_3$	9.574258	6.744128e-2	1.024908e-3	−4.207616e-5
	$\log \Delta_3$	8.030117	1.278105e-1	2.875819e-3	5.995551e-5
	$\log a_4$	7.418974e-1	−6.340965e-2	−1.805794e-3	−5.053043e-5
σ_4	$\log c_4$	1.029506e+1	6.492224e-2	1.056643e-3	−1.643501e-5
	$\log \Delta_4$	8.459989	1.137276e-1	3.515754e-3	–
	$\log a_5$	7.657208e-1	−5.775822e-2	−7.902876e-4	–
σ_5	$\log c_5$	1.073845e+1	6.189030e-2	1.130363e-3	–
	$\log \Delta_5$	8.822908	1.163591e-1	3.457547e-3	–
	a_6	2.767445	−1.126949e-1	2.483520e-3	–
σ_6	$\log c_6$	1.108196e+1	6.043375e-2	1.256963e-3	–
	$\log \Delta_6$	9.251052	1.085228e-1	1.802991e-3	–
	$\log a_7$	1.503593	6.710278e-2	1.417762e-3	–
σ_7	$\log c_7$	1.188475e+1	8.409849e-2	1.321048e-3	–
	$\log \Delta_7$	1.082135e+1	1.048287e-1	−5.310563e-3	–

Table 25. Coefficients to calculate electric conductivity according to (58).

		α_0	α_1	α_2	α_3	α_4
	$\log a_0$	1.635045	4.450390e-2	−5.928863e-4	–	–
ξ_0	$\log c_0$	5.748398	6.411299e-2	–	–	–
	$\log \Delta_0$	1.786355	−1.212690e-2	−2.375673e-4	–	–
	$\log w_0$	1.419925	−3.875497e-2	–	–	–
	$\log a_1$	4.493934e-2	−9.063708e-3	−2.489500e-3	–	–
σ_1	$\log c_1$	8.930803	5.718843e-2	1.093759e-3	–	–
	$\log \Delta_1$	7.014976	7.625175e-2	3.011941e-4	–	–
	a_2	1.593153	4.137850e-2	1.430491e-2	−4.403957e-7	–
σ_2	$\log c_2$	8.576847	1.004174e-1	7.406762e-3	−1.095186e-3	–
	$\log \Delta_2$	9.113182	−8.202725e-2	6.299430e-3	9.099828e-4	–
	$-a_3$	2.627897e-1	2.917558e-3	3.036205e-3	−1.926651e-4	−2.917018e-5
σ_3	$\log c_3$	1.023493e+1	6.651575e-2	1.090308e-3	−6.576415e-5	4.715318e-7
	$\log \Delta_3$	8.039563	1.435966e-1	8.862611e-3	−3.478227e-4	−3.614711e-5
	$-a_4$	1.707216e-1	2.035164e-2	1.809127e-3	−9.630175e-5	1.781249e-5
σ_4	$\log c_4$	1.072380e+1	5.671452e-2	1.468210e-4	2.608196e-5	6.511719e-6
	$\log \Delta_4$	8.556977	2.227207e-1	−2.773160e-3	−1.684219e-3	1.878188e-4
	$-a_5$	2.480007e-1	2.217818e-2	9.094614e-4	–	–
σ_5	$\log c_5$	1.106431e+1	5.578774e-2	6.639655e-4	–	–
	$\log \Delta_5$	9.309043	1.366510e-1	−2.599317e-3	–	–
	a_6	3.636707	−1.436268e-1	−2.934926e-3	–	–
σ_6	$\log c_6$	1.023203e+1	8.703300e-2	5.007602e-3	–	–
	$\log \Delta_6$	1.130562e+1	−2.184155e-2	−1.865543e-4	–	–
	$a_7 = a_3 + a_4 + a_5 + -a_1 - a_2 - a_6$	–	–	–	–	–
σ_7	$\log c_7$	2.946755e+1	−4.289010	−3.224136e-1	9.371814e-2	–
	$\log \Delta_7$	2.430324e+1	−2.653523	−3.309222e-1	4.769061e-2	–

Table 26. Coefficients to calculate thermal conductivity according to (59).

		α_0	α_1	α_2	α_3
a_0		−1.283401e+1	–	–	–
	a_1	1.991839e+1	–	–	–
σ_1	c_1	6.622230	–	–	–
	Δ_1	1.184624e+1	–	–	–
	$\log a_2$	7.133981e-1	−2.282818e-2	5.491632e-4	–
σ_2	$\log c_2$	2.080280	7.242844e-3	1.959358e-4	–
	$\log \Delta_2$	−1.421111	7.326017e-2	1.685275e-3	–
	$\log (-a_3)$	8.309337e-1	−2.699607e-3	2.836175e-3	–
σ_3	$\log c_3$	2.114417	6.588084e-3	1.041527e-4	–
	$\log \Delta_3$	−1.873926	7.669056e-2	4.311158e-3	–
	$\log a_4$	5.566144e-1	1.402546e-1	−4.355200e-3	1.422302e-4
σ_4	$\log c_4$	2.275814	2.789634e-3	1.613876e-4	–
	$\log \Delta_4$	−1.078759	1.962265e-2	−8.795026e-3	5.277830e-4
	$\log a_5$	−1.893687	3.628971e-2	9.796743e-3	–
σ_5	$\log c_5$	2.361178	6.072448e-3	−1.995121e-5	–
	$\log \Delta_5$	−1.820338	1.075866e-1	–	–
	$\log a_6$	1.153927	−1.647523e-2	−2.502041e-3	–
σ_6	$\log c_6$	2.467469	5.822255e-3	–	–
	$\log \Delta_6$	−2.830928e-2	−2.218935e-2	−2.718760e-3	–

		α_0	α_1	α_2	α_3
	$\log a_7$	−1.700917e+2	−2.131620e+1	−3.099200	–
γ_7	$\log c_7$	2.061427	1.117607e-3	−3.916231e-4	–
	$\log \Delta_7$	−3.290998e+1	−3.353576	−5.634466e-1	–
	$\log(-a_8)$	−1.456072e-1	−1.437036e-1	−1.480764e-3	–
γ_8	$\log c_8$	2.205458	6.659429e-3	1.324918e-4	–
	$\log \Delta_8$	−1.819779	3.825355e-3	1.202891e-3	–
	$\log a_9$	1.055279	−2.677491e-2	2.446759e-3	–
γ_9	$\log c_9$	2.183883	5.938113e-3	1.877191e-4	4.341127e-6
	$\log \Delta_9$	−9.494270e-1	3.609984e-2	1.528015e-3	−9.686251e-5
	$\log a_{10}$	2.885339e-1	−7.133722e-2	2.612269e-4	2.585150e-4
γ_{10}	$\log c_{10}$	2.255570	5.826924e-3	−5.486194e-5	−1.143664e-5
	$\log \Delta_{10}$	−1.374699	2.577156e-2	−1.763376e-3	–

Table 27. Coefficients to calculate the viscosity according to (60).

		α_0
ξ_0	a_0	−2.490318e-3
	c_0	1.138022e-5
	Δ_0	2.525477e+2
	w_0	1
σ_1	a_1	2.658346e-3
	c_1	−1.158238e+4
	Δ_1	8.370196e+3

		α_0	α_1	α_2
σ_2	$\log a_2$	−9.146259	9.214388e-2	−7.532526e-3
	$\log c_2$	8.758933	5.609203e-2	7.113878e-4
	$\log \Delta_2$	7.621521	6.802267e-2	−4.173943e-3
σ_3	$\log a_3$	−1.077843e+1	8.010183e-2	5.530383e-3
	$\log c_3$	8.183393	5.531418e-2	1.161696e-3
	$\log \Delta_3$	6.544301	1.395158e-1	1.269937e-3

		α_0	α_1	α_2	α_3	α_4	α_5
σ_4	$\log a_4$	−9.136467	4.321416e-2	−1.415683e-2	−9.589284e-4	2.418933e-4	5.834458e-6
	$\log c_4$	9.196899	6.227176e-2	1.047858e-3	−1.062417e-4	−1.844923e-6	–
	$\log \Delta_4$	7.345945	9.087033e-2	−2.859605e-3	−1.787083e-4	1.598906e-4	–
σ_5	$\log a_5$	−1.924773e-2	−1.929031e-1	−7.597965e-2	1.232504e-3	2.797944e-4	–
	$\log c_5$	1.054992e+1	6.447025e-2	−3.834145e-4	−3.294639e-5	−3.605812e-6	–
	$\log \Delta_5$	8.500778	7.811525e-2	4.703012e-3	−1.262204e-4	−1.791684e-5	–

		α_0	α_1	α_2	α_3	α_4	α_5
σ_6	$-a_6$	3.551938	−3.852851e-1	−1.698205e-2	7.712558e-4	1.558067e-4	–
	$\log c_6$	9.648995	6.284331e-2	8.307533e-4	−5.453268e-6	–	–
	$\log \Delta_6$	8.298063	8.885346e-2	−2.901675e-3	−4.450595e-4	–	–
σ_7	$\log(-a_7)$	2.202713	−5.805578e-3	−8.393797e-3	−1.542107e-4	−2.149336e-5	−3.876960e-7
	$\log c_7$	1.029898e+1	6.646081e-2	9.291080e-4	−2.151764e-5	–	–
	$\log \Delta_7$	9.012095	9.149373e-2	−3.140624e-3	−3.285520e-6	–	–
σ_8	$\log(-a_8)$	−9.551600e-1	−1.743228e-1	−2.627017e-3	2.020135e-3	1.148529e-4	–
	$\log c_8$	1.077964e+1	6.865954e-2	1.085963e-3	−3.640453e-5	–	–
	$\log \Delta_8$	8.301383	3.547869e-2	3.053608e-3	1.705129e-3	4.357310e-5	–
σ_9	$\log(-a_9)$	−4.892131e-1	3.979950e-2	2.397782e-3	−2.138908e-4	1.140375e-5	–
	$\log c_9$	1.108799e+1	5.677599e-2	4.945738e-4	−2.418338e-5	–	–
	$\log \Delta_9$	9.032754	1.718233e-1	−1.352010e-3	−2.482520e-4	1.256822e-4	–
σ_{10}	a_{10}	1.134500	−5.153304e-2	6.888543e-3	–	–	–
	$\log c_{10}$	1.144639e+1	6.234266e-2	3.785377e-3	–	–	–
	Δ_{10}	2.879605e+4	2.066908e+3	1.929331e+2	−6.651374e+1	−7.803606	–